

Effect of Addition of Al to Sn-Zn Solder Alloys

*Thesis Submitted in Partial Fulfillment of the Requirements
for the Degree of*

*Bachelor of Technology in
Metallurgical and Materials Engineering*

by

**Kapil Kumar Gupta (111MM0488)
Smarak Dash Bhattamishra (111MM0620)**

**Under the supervision
of**

Prof. S.N. Alam

Assistant Professor



Department of Metallurgical and Materials Engineering

National Institute of Technology

Rourkela-769008

CERTIFICATE

This is to certify that the work in this thesis entitled “*Effect of Addition of Al to Sn-Zn Solder Alloys*” by **Kapil Kumar Gupta** and **Smarak Dash Bhattamishra** has been carried out under my supervision in partial fulfillment of the requirements for the degree of Bachelor of Technology in Metallurgical and Materials Engineering during the session 2011- 2015 in the Department of Metallurgical and Materials Engineering, National Institute of Technology, Rourkela.

To the best of my knowledge, this work has not been submitted to any other University/Institute for the award of any degree or diploma.

Dr. S.N. Alam
(Supervisor)
Assistant Professor
Dept. of Metallurgical and Materials Engineering
National Institute of Technology Rourkela
Rourkela - 769008

A C K N O W L E D G E M E N T

We are deeply and thoroughly indebted to our supervisor, **Prof. S.N. Alam**, for being a true mentor and a guiding light, right from the commencement of this session, for his invaluable guidance, motivation, constant inspiration, and above all, for his ever co-operating attitude that enabled us in bringing up this thesis in its current form.

We give our special thanks to Prof. S.C. Mishra, the Head of the Department, for providing us with this invaluable opportunity. Our gratefulness is also due to all the faculty members of the department for helping us in any and every way possible.

We are also grateful to all the staff members of the Metallurgical and Materials Engineering department, and to all our well-wishers, branch-mates and friends for their inspiration and help. Last, but not the least, we would like to express our profound gratitude to the Almighty and our parents for their blessings and support without which this task could never have been brought to fruition.

Date - 07th May, 2015

Place- NIT Rourkela

Kapil Kumar Gupta (111MM0488)

Smarak Dash Bhattamishra (111MM0620)

8th Semester Bachelor in Technology

Department of Metallurgical and Materials Engineering

National Institute of Technology,

Rourkela-769008

ABSTRACT

Conventional solders consist of Lead, that was found to be toxic and carcinogenic. Hence, restrictions were put on its use by the industrially developed nations. To counter the use of Lead, active research was pursued into the development of Lead-free solders. In our project, we fabricated alloys of composition 3:15:82, 7:43:50 and 10:80:10 (in terms of Aluminium, Zinc and Tin respectively), under furnace cooled and air-cooled conditions. The use of Aluminium was made so as to increase the resistance of the solder to atmospheric corrosion, and also to improve the wettability of the samples. Optical micrographs were obtained for each sample so as to analyze their microstructures. For a deeper understanding, SEM images of each sample were obtained, and EDX analysis was performed side-by-side so as to understand the elemental composition of different phases present in the sample. DSC and TG tests were conducted to determine the melting point of the solder alloy, and the weight gain in the alloy on oxidation respectively. The wettability of each sample was also analyzed. We recorded and plotted down the trends in each case. We then tried to evaluate the most effective solder composition on the basis of the above tests. The near-eutectic composition was considered so as to avoid the formation of a pasty phase that will cause disruption in electrical work.

CONTENTS

1.	Introduction	8-9
2.	Literature Review	11-20
2.1	Phase Diagram	11-12
2.1.1	<i>Zn – Sn Binary System</i>	11
2.1.2	<i>Al – Sn Binary System</i>	11
2.1.3	<i>Al – Zn Binary System</i>	12
2.1.4	<i>Al – Sn – Zn Ternary System</i>	12
2.2	Literature Reviews	13-15
2.3	Literature Surveys	16-20
2.3.1	<i>Effect of Lead on Human Life</i>	16
2.3.2	<i>Lead Poisoning</i>	16
2.3.3	<i>Effect Of Lead on Environment</i>	18
2.3.4	<i>Accidental Cases</i>	18
2.3.5	<i>Legislation</i>	19
2.3.6	<i>The Role of Lead In Conventional Solders</i>	19
2.3.7	<i>The Role of Tin (Sn) In Conventional Solders</i>	19
2.3.8	<i>Discussion on The Oxidation Of Sn-Zn-Al Solder</i>	20
2.3.9	<i>Discussion on The Role Of Aluminium</i>	20
3.	Experimental Details	22-29
3.1	Materials and Methods	22
3.1.1	<i>Compositions Selected</i>	22
3.1.2	<i>Calculations</i>	22
3.1.3	<i>Sample Preparation</i>	23
3.2	Flow-Chart of the Experimental Procedure	23
3.3	Experimental Instruments	24-29
3.3.1	<i>Furnace</i>	24
3.3.2	<i>Optical Microscope</i>	24

3.3.3	<i>Field Emission Scanning Electron Microscope (FESEM)</i>	25
3.3.4	<i>Energy Dispersive X-Ray Spectroscopy (EDX)</i>	26
3.3.5	<i>Differential Scanning Calorimetry (DSC)</i>	27
3.3.6	<i>Thermo-Gravimetric Analysis (TGA)</i>	28
3.3.7	<i>Wettability Testing</i>	28
4.	Results and Discussions	31-51
4.1	<i>Optical Micrographs</i>	31
4.2	<i>SEM Images</i>	32-38
4.3	<i>EDX Analysis</i>	38-41
4.4	<i>Thermal Analysis using DSC</i>	41-46
4.5	<i>Oxidation Analysis using TGA</i>	46-50
4.6	<i>Wettability of the Solder on Cu Substrate</i>	51
5.	Conclusions	53-54
6.	References	55-56

CHAPTER-1
INTRODUCTION

1.1 Introduction:-

In today's world, Electronics and its creation is very much a vital sensation. Each contraption that we use in our day-to-day lives is ascribed to the universe of Electronics. The assembling of electronic circuits and hardware is very dependent on the procedure of Soldering.

Soldering is a procedure in which two or more metals are joined together by liquefying and streaming a filler metal into the joint, the filler metal having a generally low dissolving point described by the softening purpose of the filler metal, which is underneath 450 °C.

A solder is a fusible metal alloy used to join together metal work-pieces and having a liquefying point underneath that of the work-pieces. As opposed to shaping and adhesive bonds, soldering forms an alternate compound by chemical reaction. Some of the advantages include choice of temporary or permanent joint, joining of dissimilar metals, and flexibility in rate of cooling and heating and easy realignment.

Tin/lead solders, additionally called delicate solders, are monetarily accessible with tin concentrations somewhere around between 5% and 70% by weight. The more the tin concentration, the more prominent is the solder's ductile and shear qualities. Alloys regularly utilized for electrical binding are 60/40 Tin/lead (Sn/Pb) which dissolves at 183 °C (361 °F) and 63/37 Sn/Pb utilized primarily as a part of electrical/electronic work.

Lead, and to some degree tin, are utilized as a part of the solder, but contains little yet noteworthy measures of radioisotope contaminations. Radioisotopes experiencing alpha rot are a worry because of their propensity to bring about soft errors. In this way lead solders were discovered to be cancer-causing and subsequently securing a lead free patch have turned into a basic issue. Full use of lead free solders in commercial ventures, for example, automobiles remains a test till date. Many varieties of lead-free solders have been used, but there are issues such as poor mechanical properties, higher melting points etc. Sn–Ag solders have been viewed as the most encouraging alternative to supplant Sn–Pb welds later on, yet the dependability and expense issues are considerable. The Sn-Zn eutectic composition has as of late been considered as a contender for a lead-free bind as a result of its low softening point (198°C), incredible mechanical properties and minimal cost.

One of real disadvantages of soldering is that the careful evacuation of the flux residuals is needed to avert corrosion. In this way, we incorporated an ideal temperature solder with a melting point of 199°C by joining aluminum (Al) to Sn-Zn-based material to improve corrosion resistance, and help decrease its oxidization.

The samples prepared are assessed from the perspective of physical, mechanical, structural and chemical properties.

CHAPTER-2
LITERATURE REVIEW

2.1 Phase Diagram

2.1.1 Zn – Sn binary System

The Zn-Sn binary system is a simple eutectic system. The eutectic reaction takes place at the temperature of 198.5°C in the alloy containing 85.1 % Sn.

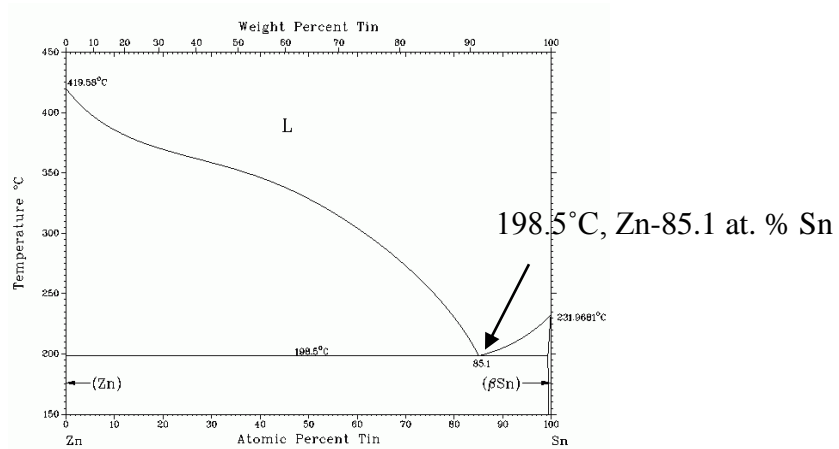


Figure 1-Zn-Sn phase diagram

2.1.2 Al – Sn binary System

The Al-Sn binary system is of the simple eutectic type. The eutectic reaction takes place at the temperature of 228.5°C in the alloy containing 97.6 % Sn.

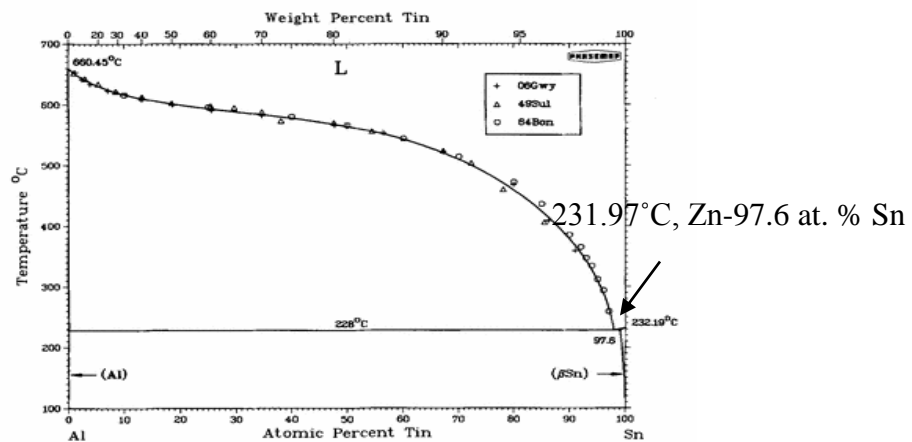


Figure 2-Al-Sn phase diagram

2.1.3 Al – Zn binary System

The equilibrium phase Diagram of Al-Zn is a eutectic system involving a monotectoid reaction. The eutectic reaction proceeds at 381 °C close to the Zinc side (eutectic point has 88.7 % Zinc). The monotectoid reaction occurs at the temperature of 277 °C.

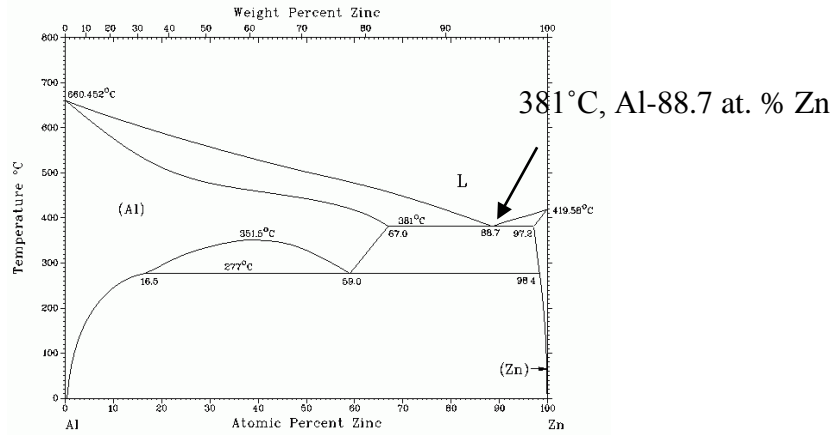


Figure 3-Al-Zn phase diagram

2.1.4 Al – Sn – Zn ternary system

The diagram of the Al – Sn – Zn ternary system was published in various journals. 93 alloys, which were prepared by melting 99.995% Al, and 99.933% Sn and 99.99% Zn in an argon atmosphere, were thermally analysed by Prowans et al. Determination of the three vertical sections, as well as the solidus surface and the liquidus surface was done. Zone melting was used to determine the ternary eutectic composition.

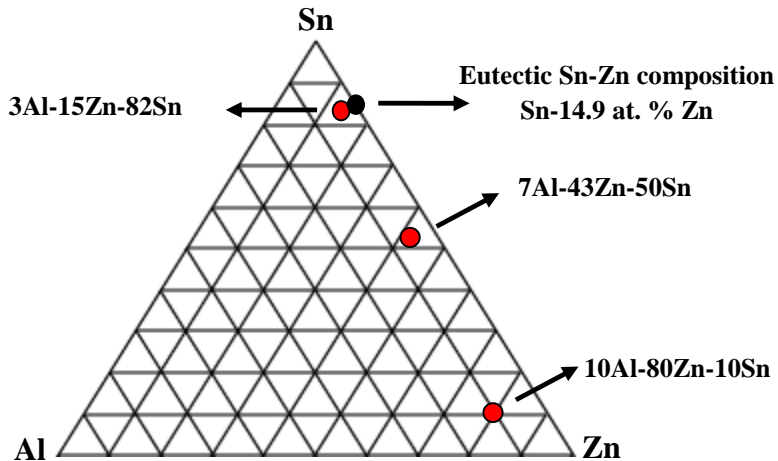


Figure 4-Al-Zn-Sn ternary phase diagram

2.2 Literature Reviews

Kitajima et al. said about the harmful effects of lead in conventional lead-based solders. As one of the pioneers in the development of alternative solders, they suggested the use of a Sn-Zn-Al eutectic. They found the melting point of the said compound to be close to the conventional lead solders. They also investigated and found the joint reliability of these solders to be acceptable for industrial use. They found that on a little addition of Al, corrosion resistance and wetting properties improve.

Pu Yu et al. studied an eutectic alloy (composition: 91Sn-9(5Al-Zn)), and investigated the formation of intermetallics (IMC) with a Cu substrate. They found the IMC to be γ -Cu₅Zn₈, which develops at the alloy-Cu interface. They found that between the Sn-Zn-Al solder and the Cu substrate, the adhesion strength decreased from 6 ± 0.7 to 4.8 ± 0.6 MPa as the heating time increased to 250 h at 423 K.

Drapala et al. carried out preliminary study of Al – Sn – Zn system. They discovered that long-term annealing is necessary, which should be followed by structural and chemical microanalysis of the phases and their concentration limits.

Lin et al. investigated and found that the eutectic reaction of the Sn-Zn-Al system occurs at about 200°C. Eutectic behavior was exhibited by 91Sn-8.55-Zn-0.45Al solder during cooling. A precipitate (composition 39.2Zn-35.1Al-25.7Sn (Al₆Zn₃Sn)) forms in the solder. The primary phase is Sn-(5.41~12.0)Al-(3.19~5.77)Zn, and the secondary phase is Sn-1.36Zn-0.33Al. An increase in the Al and Zn contents complicates the cooling behavior and microstructure of the solders.

Luo et al. investigated Sn-xAg-1Zn solders, and found that on the addition of Ag, liquidus rises and pasty range enlarges. On increasing Zn content, the liquidus can be reduced at varying Ag

contents, though the addition of excessive Zn may cause sharp fall of solidus, even leading to formation of Sn–Zn eutectic. The optimized composition at varying Ag content are Sn–1Ag–2Zn, Sn–1.5Ag–2Zn and Sn–2Ag–2.5Zn respectively.

Song et al. investigated the effects of addition of Ag content on microstructural and vibrational deformation properties of lead-free solder. These additions result in the formation of Sn-rich dendrites and Ag–Zn IMC (ϵ -AgZn₃), which substitute the Zn-rich phase. The low-Ag samples with a Sn–Zn eutectic structure have poor damping capacities and shorter vibrational life. In comparison, wavy-striated deformation of Sn-rich dendrites occurring during vibration may be regarded as a proper mechanism for absorbing vibrational energy. Therefore, the specimens with Ag content greater than 1.5 wt% exhibit greater damping capacity and longer vibrational life than low-Ag specimens.

Liu et al. investigated the microstructures under varying cooling rates (0.16 K/s, 100 K/s and about 10000 K/s). They found uniform microstructures and fine IMC particles, even some nano-sized Ag₃Sn, existing in the slowly-cooled and water-cooled Sn–3.7Ag–0.9Zn solder. At high cooling rates (about 10000 K/s), Sn dendrites form easily in the Sn–3.7Ag–0.9Zn solder, and ternary Ag–Zn IMC separate along the grain boundary of the dendrites post-annealing.

Hung et al. investigated the structural properties and tensile characteristics of Sn–9Zn–*x*Ag alloy under electrical current testing and oil-bath treatment. For the Sn–9Zn–*x*Ag alloy, Ag–Zn compounds flourished, Zn-rich phases and Sn–Zn eutectic decreased. On the addition of a further 2 wt.% Ag into Sn–9Zn alloy, changes in electrical conductivity occurred. No microstructural changes occurred during oil-bath heat treatment, but a phase transformation was caused due to thermoelectric effect, causing the following changes: Ag–Zn compounds and Sn–Zn eutectic phase increased, and Sn-rich phase fell. Increasing the period of the thermo-electric effect resulted in the tensile and mechanical properties to deteriorate. Increasing the oil-bath temperature strengthened the solid-solution effect and increased the tensile strength.

Vaynman et al. discussed the use of computational thermodynamics on the design of lead-free solders. It is shown that the earlier reported Sn-9 mass%Zn-5 mass% In is not an optimum composition, with respect to the melting temperature, the solidification range and the solid-solid phase transformations. Long-time exposure of the Sn-Zn eutectic solder in very severely accelerated test (85% relative humidity at 358 K) for six weeks did not adversely affect the mechanical properties. The shear stress-strain properties of Sn-Zn eutectic solder are not affected by the exposure.

Pstrus et al. investigated the wetting properties of Cu and Al by Sn-Zn eutectic. The wettability problems due to the presence of ZnO or Al₂O₃ at the solder-pad interface, were eliminated by appropriate preparation of substrates by using an appropriate flux and atmosphere, along with proper choice of soldering temperature. Such alloys may be used for soldering of both Cu and Al. Spreading tests concluded that wetting properties of solders based on Sn-Zn on copper pads don't depend on the temperature (up to 673 K), but due to the lack of a protective atmosphere, the solder doesn't wet the pads.

Yu et al. also investigated the interfacial microstructure and wetting property of Sn-Zn-Cu solders with a Cu substrate. They determined the compositions of the IMCs on the surface by EDS. With the rise of Cu content in the solder, the Cu and Sn concentration in the intermetallic layer gets higher and the Zn content goes lower. On the surface of Sn-9Zn/Cu, Cu₅Zn₈ compound morphology shows a granular appearance.

Bian et al. investigated liquid structures of Cu-Al and Al-Ni. They reported that if IMC forms in the alloys, there exists not only a short-range ordered structure, but also a medium-range order (MRO) in the liquid metal, under certain considerations. The temperature has a huge effect on the creation of the MRO structure. As per the Cu-Zn binary diagram, Zn-Cu IMC form in a wide range. Therefore, a possible formation of SRO Cu-Zn structure in the liquid solder occurs as the soldering temperature is only 30-60 K more than the melting temperature.

2.3 Literature Surveys

2.3.1 Effect of lead on human life

As per Environment Protection Agency (EPA), lead (Pb), and its compounds are some of the top chemicals posing a threat to human life. When Pb comes in to contact with the human body, it associates with the proteins in the body over a period of time, and decelerates their usual functions. If the lead amount in blood cells is higher than allowed concentration, lead poisoning may occur. While considering the case of soldering operations, Pb contamination may not be a large problem, since at the soldering temperature, Pb is less volatile. However, the ingestion of Pb vapour and the dust formed during wave-soldering process may have deleterious effects on human health. During wave-soldering operation, dross-formation is expected due to oxidation reactions at the surface of the molten solder. 90% of the dross can be refined for reuse, but the remaining 10% is useless. The Resource Conservation and Recovery Act (USA) specifies that this waste may be damaging to human health, and hence, proper care and disposal must be carried out.

2.3.2 Lead Poisoning

It is a form of metal poisoning causing a medical condition resulting from high levels of the heavy metal lead in the body. Pb interferes with different body processes. It is toxic to vital organs and tissues, which include the heart, intestines, bones, reproductive system, nervous system and kidneys. It is particularly deleterious to children, causing permanent learning and behavioural disorders. Symptoms may include abdominal pain, anemia, irritability, confusion, headache, and in extreme cases, seizures, coma, and, even death.

Routes of lead exposure consist of contaminated soil, food, air, water, and consumer products. Occupational exposure is a common cause of lead poisoning in adults. As per estimates given by the National Institute of Occupational Safety and Health (NIOSH), greater than 3 million workers in the US are potentially exposed to Pb in their workplace. A great threat to children is the lead paint in many homes.

Sources of exposure: Significant routes of Pb poisoning include industrial use (Pb-acid batteries, wire and pipes, electronic components), foundries and metal recycling. It can also result from contaminated water through lead pipes, and from soil and air. There are different ways of solid lead contamination, which includes residues from lead, waste landfills, used engine oil, or from smelter plants. Water supply pipes made of lead, or on which lead solder joints have been made, pose a high level of danger. The amount of lead in water depends on the acidic nature, temperature, standing time of water and water hardness. It has been deduced that, in the USA, 14-20 % of the total lead poisoning has been caused by drinking water. In 2004, an article published about lead concentration in drinking water in “The Washington Post” was awarded. The name of this article was-“How lead toxicity affects human health?” After being absorbed, Pb bonds with the proteins and enzymes in the human body. It travels in the blood and attacks the soft tissues majorly. After some days, most of the Pb moves to the teeth and to the bone marrow. In the adults, 94 % of the total Pb concentration is present in the bones and the teeth, while in children, 73 % of the total Pb content is in the bone marrow.

(a)Renal system

Here, failure can be caused by high levels of Pb in the human blood cells. It can result in *Fanconi Syndrome*, which stops the normal functioning of the kidneys.

(b)Cardiovascular failure

Pb exposure may result in heart rate variability, coronary heart disease, high blood pressure and even in heart attack.

(c)Reproductive system

Both female and male reproductive systems are damaged by lead poisoning. In the case of men, sperm count heavily decreases where the lead concentration is greater than 40 µg/dl. It is even more dangerous in the case of pregnant women, since the high blood-lead levels can lead to prematurity, miscarriage, may even be harmful to the baby.

(d)Nervous system

As a result of lead poisoning, the nerve cells degenerate and lose their usual functions (relating to response to the stimuli). Lead passes through the layer of endothelial cells, because it resembles the Ca ions. Inside the developing brain of a child, Pb slows down the synapse-formation inside the cerebral cortex. It reduces the number of neurons, affecting neurotransmission and reducing neuronal growth.

2.3.3 Effect of lead on environment

The disposal of waste electrical/electronic assemblies containing lead (or its compounds) is considered deleterious to the environment. The lead-containing components are dumped in solid-waste landfills. They contaminate the ground water. Usual purification processes are not usable for removal of Pb. Actually, it is difficult to explain bond formation between lead and water. However, a study has proven that PbO converts to PbCO₃ in the presence of CO₂ and Cl. USA and Japan are considered to be the two largest suppliers and users of printed circuit board (PCB) assemblies. Current studies have shown that this market will double in the coming 10 years. Hence, proper disposal of Pb-containing components is not a small issue. Recycling of lead seems to be a major solution to this problem. However, the use of recycled Pb is limited. It has been proven that recycled Pb shows higher α -particle emissions than pure Pb, and this hampers the performance of circuits

The lead level is increasing fast due to rapid industrialization during the last few years. Pb content of 0.003 mg/l in water is regarded to be normal and non-hazardous to the ecosystem. In India, many rivers have been found to be polluted with large amounts of Pb. The water of the famous Hussain Sagar lake is probably polluted by industrial waste from the city. During the “Green Revolution”, the higher use of lead-containing pesticides in Punjab and Haryana resulted in water and soil contamination to a very high level. Plants absorb lead-contaminated water through their roots. In plants, Pb toxicity depends upon the absorption, transportation and intra-cellular localization. It has been seen that plants in urban areas are more prone to Pb poisoning. Pb reacts with relevant functional groups and slows down their normal operations, many of which help in photosynthesis and the assimilation of nitrogen. Many tests have been carried out on animals, too. They show that Pb poisoning affects animals, and the symptoms are almost similar to that of the human race, like peripheral neuropathy and abdominal pain.

2.3.4 Accidental cases

- 1) In Nigeria, on October 5, 2010, more than 400 children died due to Pb poisoning (this is referred to as the Zamafara state lead poisoning epidemic).
- 2) In China, more than a 1000 children from about 10 different villages residing near the Yuguang gold-and-lead smelter plant were reported to show excess blood-lead level. After

this incident, around 15000 people from the area relocated to other areas. The Government has since stopped the production of Pb from 32 Pb plants.

2.3.5 Legislation

On October 11, 2002, the European Community Members (currently Germany, Italy, Denmark, Belgium, Finland, France, Portugal, Sweden, Greece, Spain, Holland and the UK) forbade the usage of some dangerous substances in electrical/electronic equipments. It was decided that four heavy metals (cadmium, mercury, hexavalent chromium and lead) will not be used any further from 1 January 2004. In USA, laws were introduced regarding the elimination of lead. In Japan, though the use of lead has not been banned yet, however their laws forbid Pb from being sent to landfills and other waste-disposal yards. Many Japanese companies have started acting on this, and have set their own methods for creating Pb-free equipments. Since March 2002, Seiko Epson Corporation has stopped using Pb- bearing solders in PCBs and other components. In India, as of now, there is no concrete legislation on this issue. But given the potential hazards, greater care has to be taken now.

2.3.6 The role of lead in conventional solders

Lead is comparatively cheap and very widely available. The conventional soldering alloys which are based on the eutectic or near-eutectic compositions of the Tin-Lead system have been studied and analyzed with a wide array of research. Sn-37Pb (eutectic composition) and Sn-40Pb are the mainly used solders in electronic industries.

Lead in solders gave the following advantages:-

1. Pb reduces the surface tension of pure Sn, and hence facilitates wetting.
2. Pb acts as solvent, and allows other metals such as Cu and Sn to form IMCs by diffusion.
3. Pb stops the transformation of white Tin in to gray Tin on cooling. This transformation causes an increase in the volume, and adversely affects the structural properties of Sn.

2.3.7 The role of tin (Sn) in conventional solders

White (Sn) converts to gray Sn if it is kept for a longer period of time at a temperature less than 273K. The temperature for transformation between the two phases is 286K. It is interesting to

observe that metal (white tin) converts to semiconductor (gray tin), with a volume increase (27%). Sn easily wets and spreads on the substrate. This results in Sn being a major constituent in most solder alloys. However, the aforementioned transformation results in problems in devices which cycle across 286K. Under repeated thermal cycling, plastic deformation, and subsequent crack formation are result even without external load. In accordance with earlier works, Aluminum, Zinc, Germanium and Copper enhance gray Tin formation, while Antimony, Cadmium, Bismuth and Lead have a negative effect on the transformation. The whiskers are tetragonal white tin (β -tin), which grow due to internal stresses and strains. Whiskers don't affect soldering-ability, but longer whiskers may result in short-circuits in PCB assemblies. It has been seen that on addition of lead, the whisker growth seen in tin is suppressed.

2.3.8 Discussion on the oxidation of Sn-Zn-Al solder

The addition of Al improves the wettability of a Sn-Zn solder considerably. The reason for the preferential oxidation of Al over Zn in the solder is due to the difference in relative affinities towards oxygen. As Zn absorbs oxygen and forms a ZnO layer on the surface, the oxygen molecules keep entering the porous layer of ZnO, and as a result, the oxide layer thickness increases. Therefore, the wetting power of the solder reduces significantly.

2.3.9 Discussion on the role of Aluminium

When Al atoms are added, they come in to contact with air, and formation of a thick Al₂O₃ layer occurs. It is well-known that Al atoms are prone to partially release electrons as a result of their chemical properties, and hence react with the oxygen molecules. The segregation of Aluminium atoms in the solder prevents contamination of Zinc by oxygen. Electron-releasing Aluminium atoms are constantly provided to the metal surface, and as a result, an interface is maintained between the oxygen molecules and the metal surface on the positive and the negative sides, respectively.

Furthermore, because of the Al₂O₃ oxide film, moisture entry is restricted, and hence corrosion resistance improves.

CHAPTER-3
EXPERIMENTAL DETAILS

3.1 Materials and Method

3.1.1 Compositions Selected

We procured Al power, Sn & Zn granules and prepared seven samples of composition as follows :-

COMPOSITION	Al (at %)	Sn (at %)	Zn (at %)
Sample 1 (eutectic)	0	85.1	14.9
Sample 2 (furnace cooled)	3	82	15
Sample 3 (Air Cooled)	3	82	15
Sample 4 (furnace cooled)	7	50	43
Sample 5 (Air Cooled)	7	50	43
Sample 6 (furnace cooled)	10	10	80
Sample 7 (Air Cooled)	10	10	80

3.1.2 Calculations

How weights were calculated for creating a sample:

Let us consider the case of 3 Al-15 Zn-82 Sn solder alloy sample. The given proportions are representative of the atomic weight percent of each constituent element. This atomic weight percent was converted to mass by using the following method:

1. For every 100 atoms, we have 3 Al atoms, 15 Zn atoms and 82 Sn atoms.a
2. This implies that for every 0.1 atoms, there are 0.003 Al atoms, 0.015 Zn atoms and 0.082 Sn atoms.
3. Now we multiply these values with the corresponding molar mass for each element (Al-27, Zn-65.4, Sn-118.7). We get the results as:
 - a. Mass of Al=0.081 g
 - b. Mass of Zn=0.981 g
 - c. Mass of Sn=9.73 g

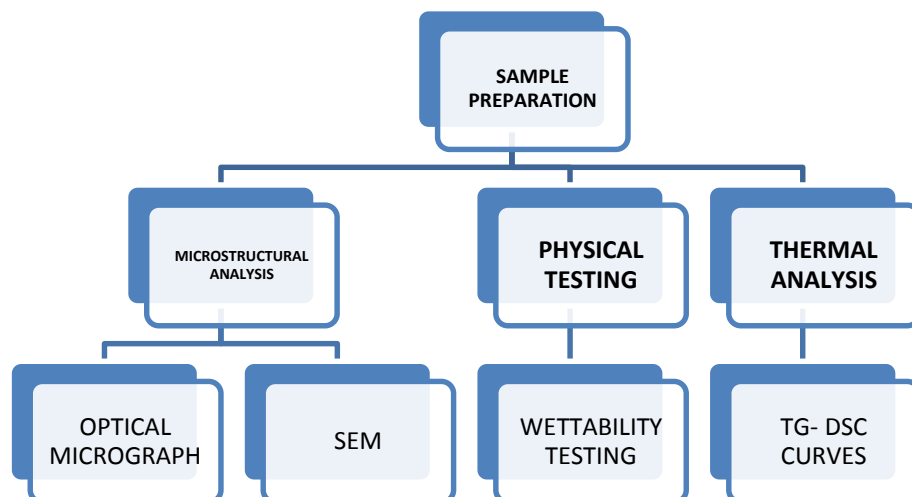
We similarly calculate the weight values for the other solder alloy samples.

3.1.3 Sample preparation

The process of sample preparation is given as follows:-

- 1) Calculated weights of Al, Zn and Sn were taken, two times (one each for furnace-cooling and air-cooling respectively).
- 2) First, Sn was emptied in to the silica crucibles, and put inside the furnace. The temperature was set at 673K to ensure complete melting of Sn.
- 3) The crucibles were then carefully taken out, and Zn chips of the given weight were added. The crucibles were then put back inside, and the temperature was set at 773K. The crucibles were allowed to stay inside for some time to ensure proper melting of the mixture.
- 4) Then, the crucibles were again carefully taken out, and the calculated weight of Al powder was added to the crucibles. The crucibles were now put back in to the furnace, and the temperature is set at 973K to melt and homogenize the mixture.
- 5) The samples were allowed to soak at that temperature for about 2 hours, after which the furnace was switched-off.
- 6) For each sample, one crucible was allowed to stay in the furnace for furnace-cooling, and the other is taken out for air-cooling.
- 7) The samples were collected the next day.

3.2 Flow-chart of the experimental procedure



3.3 Experimental Instruments

3.3.1 Furnace

It is a closed chamber, which is used for the heating via convection, radiation and conduction. The energy supplied is given by fuel combustion, by the use of electricity or through the use of heating in the induction furnaces. An example is the muffle furnace (also known as retort furnace); here, the material is heated under stringent temperature conditions imposed with the use of a thermocouple. Here, the heating, the soaking and the cooling trends are attained by manual operation of the control panel.

Some of the advantages include

1. Greater control over temperature
2. Isolation of the material that is being heated



Figure 5-A muffle furnace

3.3.2 Optical Microscope

This is the simplest form of imaging. Here, visible light and a system of different lenses are used to magnify images. The images are captured by the light-sensitive cameras, and as a result, a micrograph is generated. The components include an eyepiece, an objective turret to hold the objective lenses, the focus knobs, a stage and a light source. The power or magnification of the compound optical microscope is given by the product of the powers of the ocular and the objective lenses. The maximum normal magnifications of the lenses are $10\times$ and $100\times$ respectively, hence giving a total final magnification= $1,000\times$.



Figure 6-An Optical Microscope

3.3.3 Field Emission Scanning Electron Microscope (FESEM)

A FESEM is a microscope that uses electrons instead of light. The electrons are freed by a field emission source. The given specimen is scanned by these electrons in a zig-zag pattern. The resolution is in the range of around 10 nanometers. The microscope operates at magnifications ranging from 10 to 300,000. In addition to giving topographical information (as is done by optical microscopes), it also provides information about the chemical composition in the surface. Here, a source of electrons is concentrated in to a beam, which has a very fine spot size of **5 nm** and has energy in the range of 50Kev to a few hundred eV, that is spread over the surface by making use of deflection coils. Different interactions occur between the surface and the electron- beam, as the beam hits and penetrates the surface, resulting in the production of electrons and photons. Images produced form on the cathode ray tube (CRT). The varieties of images produced in **SEM** are:

1. Secondary (SE) electron images,
2. Backscattered (BSE) electron images
3. X-ray elemental maps

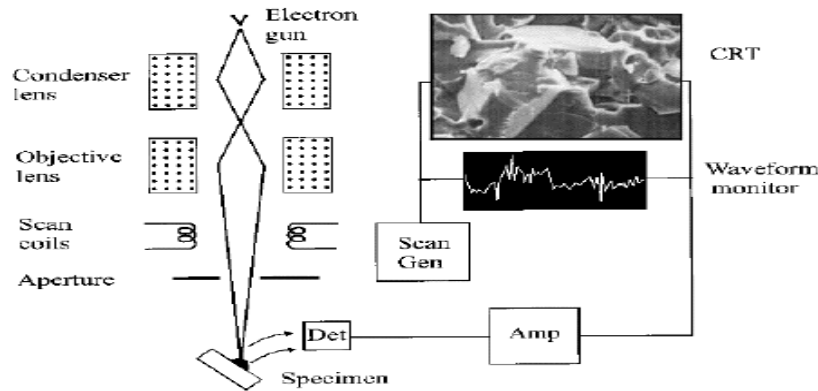


Figure 7-Schematic representation of Field Emission Scanning Electron Microscope



Figure 8.-A typical FESEM set-up/SEM

3.3.4 Energy Dispersive X-ray spectroscopy (EDX)

Here, the principle is that X-rays enter the energy dispersive spectrometer through a thin Beryllium window, and create electron-hole pairs inside the semiconductor crystals. The mechanism includes a fast beam of electrons, which have an energy high enough to excite all the atoms present in the periodic table. Then, the ionization of electrons from the K, L, and M shells occurs. As a result of de-excitation, we obtain X-rays.

- The important uses can be classified in to:

- **Qualitative-** here, X-rays are used to identify different elements

- **Quantitative-** here, integrated peak intensity is used to determine the amounts of different elements.

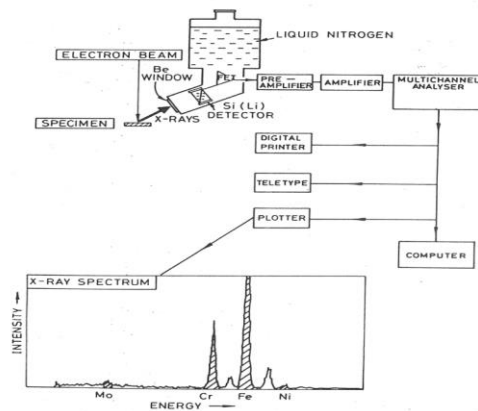


Figure 9-schematic representation of the Energy Dispersive X-Ray spectroscopy process

3.3.5 Differential Scanning Calorimetry (DSC)

This is a method of thermal analysis dealing with the change in heat capacity (C_p), with respect to the change in temperature. Both the sample substance and the reference substance are compared by keeping them in different chambers. The variation in heat capacity as similar to the change in the heat flow is calculated, when the sample of a known mass is either heated or cooled. The examples of the different types of data that can be deduced are – the melting temperature, the phase change, the glass transition temperature and the curing temperature.



Figure 10- A standard Differential Scanning Calorimetry Set-up

3.3.6 Thermo-gravimetric analysis (TGA)

It is a method of thermal analysis, whereby changes in the chemical and physical properties are studied as a function of temperature (with a constant heating rate), or as a function of time (with a constant temperature and/or a constant mass loss). Common applications of TGA include:-

1. Study of mechanisms of degradation
2. Study of reaction kinetics
3. Material characterization
4. Analysis of organic content (like ash) in a specimen

3.3.7 Wettability

Experimentally, it has been observed that liquids placed on solid surfaces usually do not completely wet, but, rather, remain as a drop that has a definite contact angle between the liquid and solid phases. This condition is illustrated in Fig. The Young and Dupré equation permits the determination of change in surface free energy, ΔF , accompanying a small change in solid surface covered, ΔA .

The contact angle is the angle, conventionally measured through the liquid, where a liquid/vapor interface meets a solid surface. It quantifies the wettability of a solid surface by a liquid via the Young equation. A given system of solid, liquid, and vapor at a given temperature and pressure has a unique equilibrium contact angle. However, in practice contact angle hysteresis is observed, ranging from the so-called advancing (maximal) contact angle to the receding (minimal) contact angle. The equilibrium contact is within those values, and can be calculated from them. The equilibrium contact angle reflects the relative strength of the liquid, solid, and vapor molecular interaction.

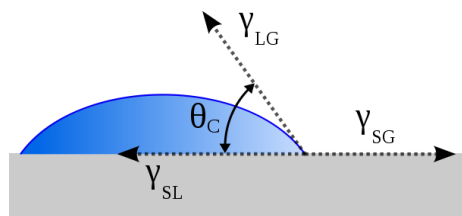


Figure 11-Schematic representation of wetting of a liquid bubble on a solid substrate

The theoretical description of contact arises from the consideration of a thermodynamic equilibrium between the three phases: the liquid phase (L), the solid phase (S), and the gas/vapour phase (G) (which could be a mixture of ambient atmosphere and an equilibrium concentration of the liquid vapour). The “gaseous” phase could also be another (immiscible) liquid phase.

$$\gamma_{SL} = \gamma_{SV} - \gamma_{LV} \cos(\theta) \quad \dots(1)$$

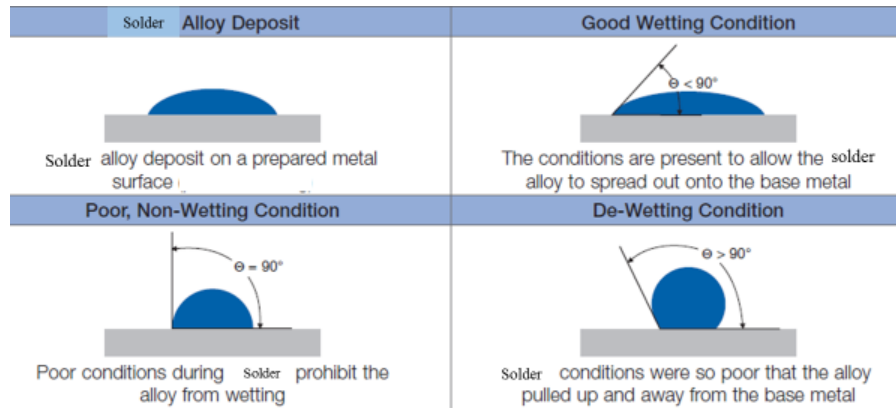


Figure 12-Schematic representation of wetting of solder alloy on Cu substrate

CHAPTER-4
RESULTS AND DISCUSSION

4.1 Optical Micrographs

4.1.1 Sn- Zn Eutectic Alloy (sample 1)

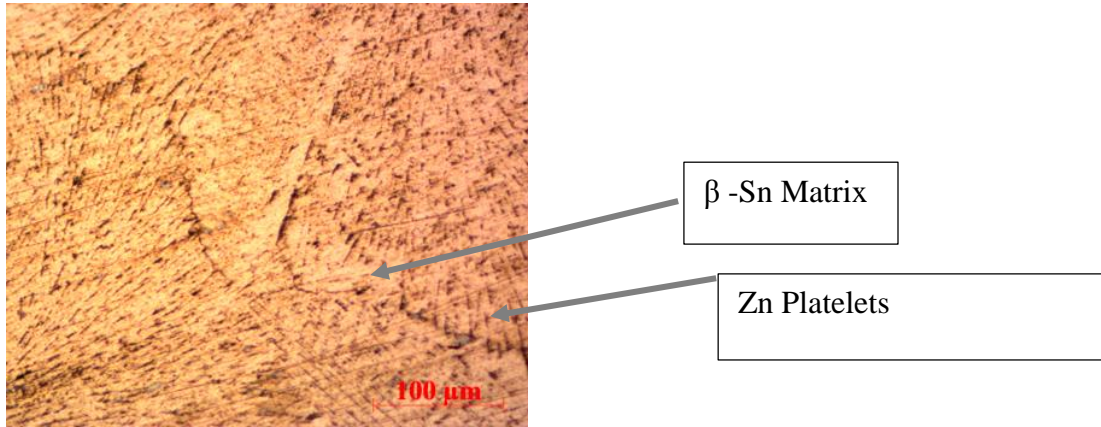


Figure 13-Micrograph of Sn-Zn eutectic alloy

Sn–14.9Zn (at %) alloy shows simple structure with a Zn-rich phase. This phase is homogeneously dispersed in the β-Sn matrix.

The normal microstructure of Sn–Zn eutectic is that Zn is distributed in Sn matrix as platelets.

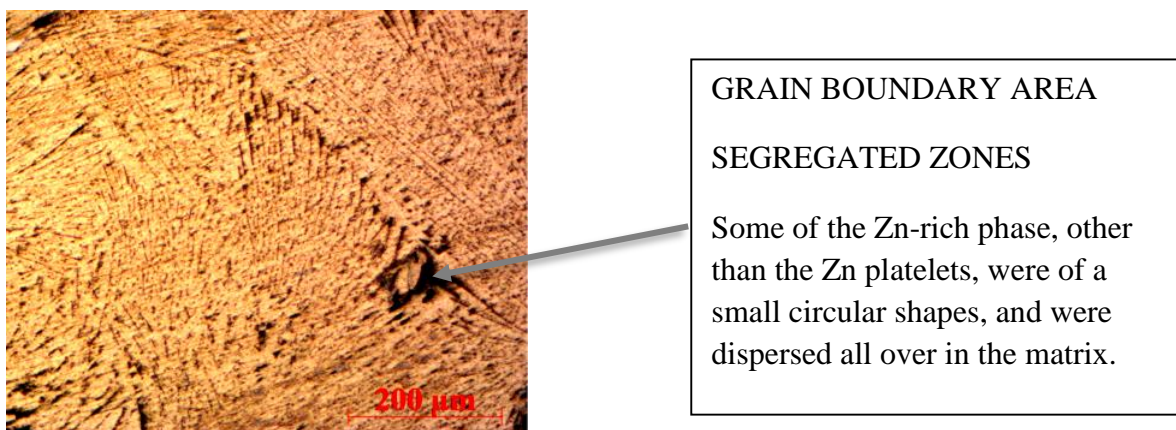


Figure 14- Micrograph of showing the grain boundary region

4.2 SEM Images

4.2.1 Sn- Zn Eutectic Alloy (sample 1)

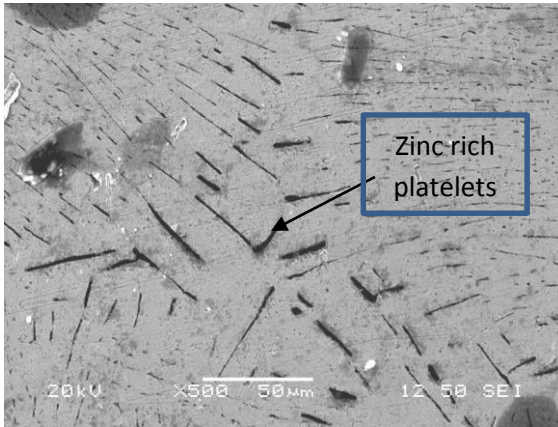


Figure 15-Low magnification image of Sn-Zn eutectic alloy

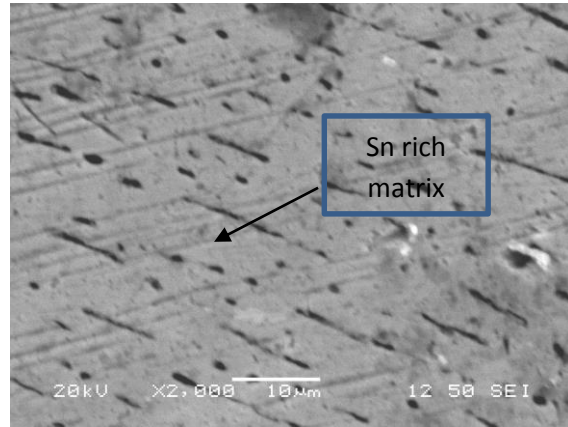


Figure 16-High magnification image of Sn-Zn eutectic alloy

Sn-14.9Zn (at %) alloy shows simple structure with a Zn-rich phase. This phase is homogeneously dispersed in the β -Sn matrix. The normal microstructure of Sn-Zn eutectic is that Zn is distributed in Sn matrix as platelets.

4.2.2 82Sn-15Zn-3Al (furnace cooled) solder alloy (sample 2)

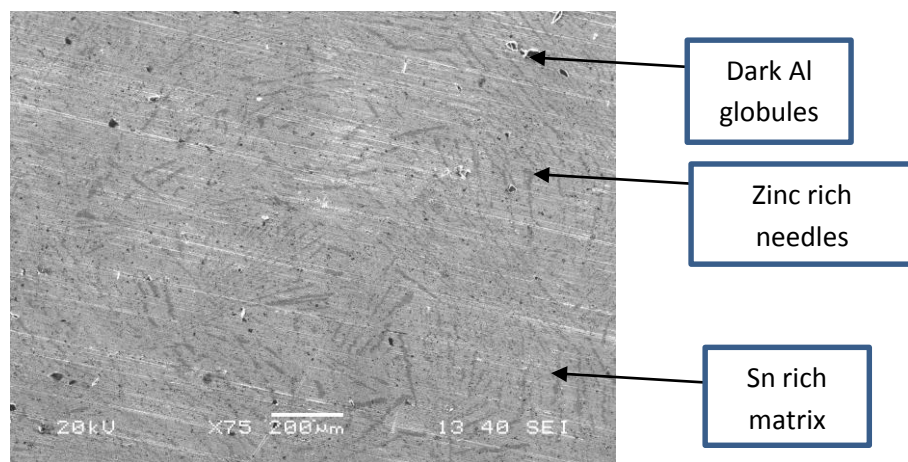


Figure 17-82Sn-15Zn-3Al (furnace cooled) solder alloy at low magnification

Fig. shows the microstructure of the 82Sn-15Zn-3Al solder alloy. The phase having the lighter contrast is that of β -Sn and the dark needle-like phase is the Zn-rich phase. The addition of 3 atomic % Al to the Sn-Zn eutectic alloy gives rise to precipitation of the Al-rich phase with a near diamond shape. The 82Sn-15Zn-3Al solder alloy on cooling undergoes the reaction,

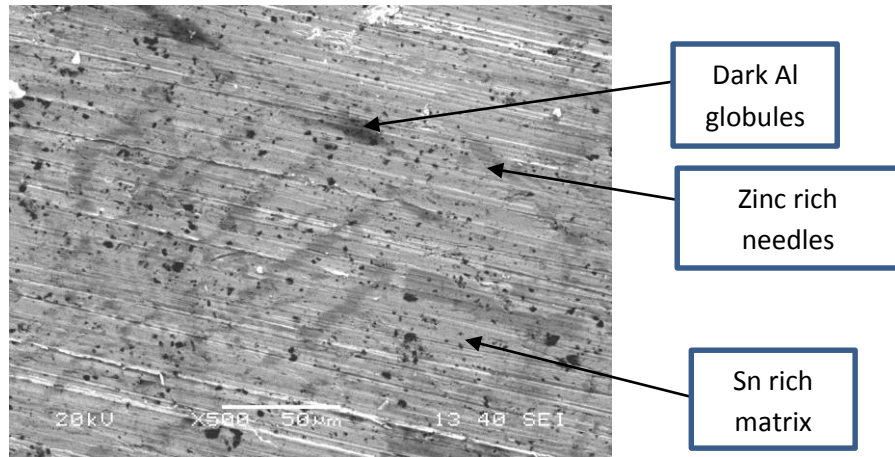


Figure 18-82Sn-15Zn-3Al (furnace cooled) solder alloy at high magnification

The solubility of Sn in Al is very poor, with a maximum of approximately 0.026 atomic % Sn dissolving at around 625°C. Segregation of Al rich phase takes place as the liquid solder alloy is cooled below the eutectic temperature. The dark coloured needle-like Zn-rich phase precipitates are dispersed in the light coloured Sn rich matrix. The overall microstructure is very similar to that of the Sn-14.9 at. % Zn (8.8wt. % Zn) eutectic alloy. The SEM micrograph of the 3Al-15Zn-82Sn furnace cooled alloy indicates a typical lamella eutectic microstructure.

4.2.3 82Sn-15Zn-3Al (Air cooled) solder alloy (sample 3)

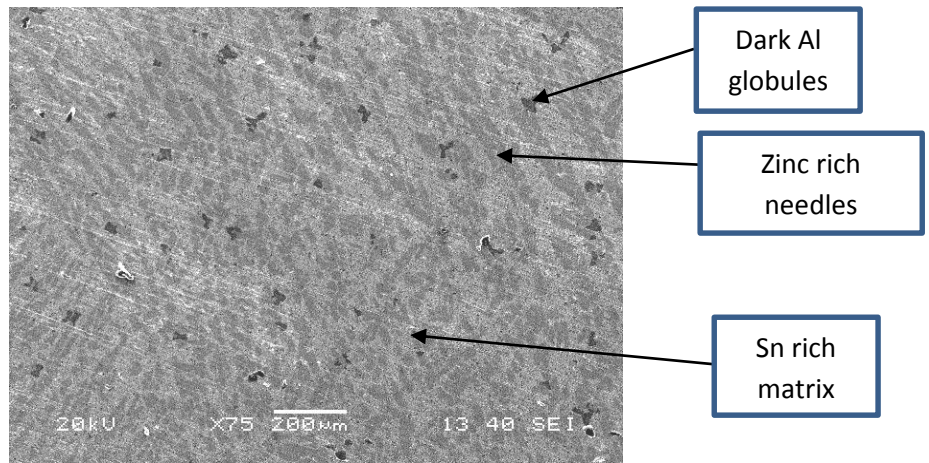


Figure 19-82Sn-15Zn-3Al (Air cooled) solder alloy at low magnification

Here, SEM indicates a typical lamellar microstructure which is characteristic of the eutectic composition. The light coloured background is the secondarily solidified Sn rich phase. This is reasonable as the phase with greater contents of Al and Zn is expected to solidify first. The volume percent of the dark coloured Zn-rich regions is low due to the high Sn content in 3Al-15Zn-82Sn alloy.

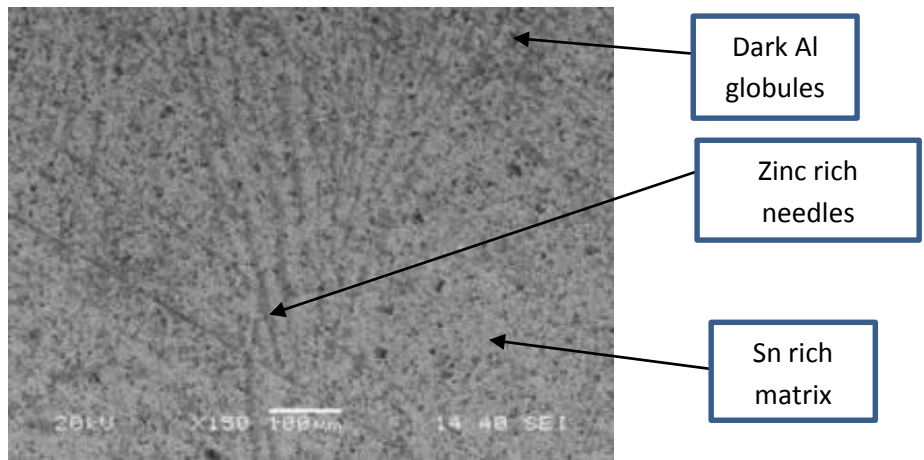


Figure 20-82Sn-15Zn-3Al (Air cooled) solder alloy at higher magnification

For the eutectic composition containing Sn-14.9 at. % Zn the eutectic reaction takes place at the temperature of 198.5°C. The alloy 3Al-15Zn-82Sn is a near eutectic composition and this is why the microstructure is very similar to that of the eutectic alloy.

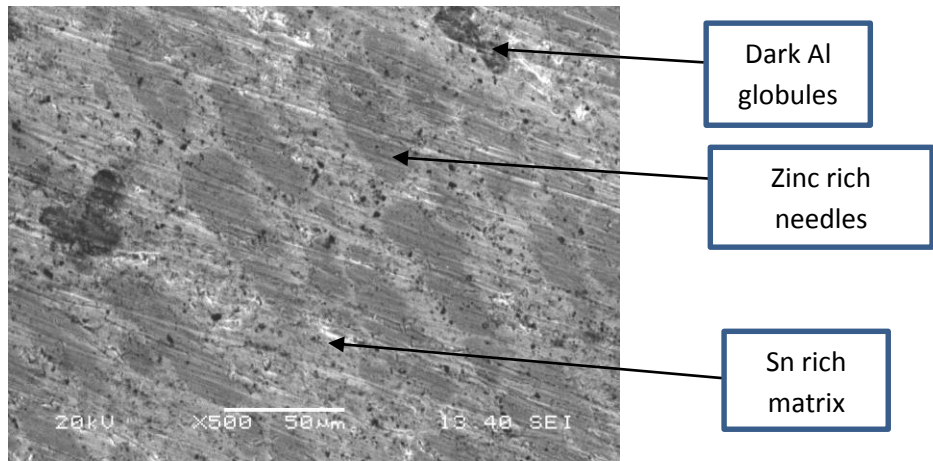


Figure 21-82Sn-15Zn-3Al (Air cooled) solder alloy at very high magnification

From this figure it is evident that there is decrease in the grain size and the increase in size and number of zinc globules present which is because of the higher rate of cooling than in furnace cooled sample. Because of the higher rate of cooling than furnace cooling, the time for diffusion decreases and thus instead of forming platelets the zinc segregates as a globules. Since the rate is not very high (like quenching) thus Zn platelets are also found in the matrix.

4.2.4 50Sn-43Zn-7Al (furnace cooled) solder alloy (sample 4)

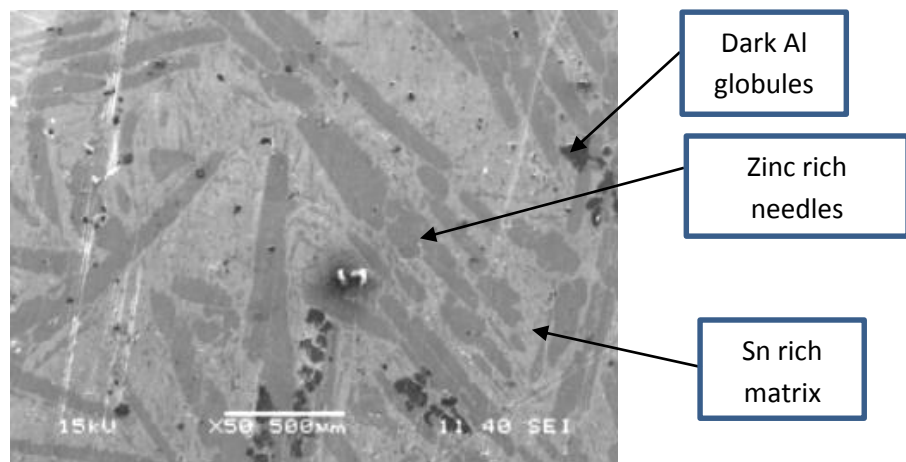


Figure 22-50Sn-43Zn-7Al (furnace cooled) solder alloy at low magnification

SEM image of Sample 1, 2 and sample 3 consists of a eutectic lamellar structure while sample 4 consists of a dendritic structure. This is evident from the composition difference between the samples as the former being close to eutectic composition of binary Sn-Zn system.

SEM analysis shows considerable heterogeneity of microstructure which will relate to the formation of non-equilibrium phases in the course of solidification. Mostly two or three types of phases of various chemical compositions were discovered.

The three phases were

Small Black phases (A) - Contain high concentration of Aluminum + Zinc and a certain concentration of Oxygen

Grey phase (B) – Contain high concentration of Zinc without Tin.

White phase (C) - Contain high concentration of Tin without Aluminum

The primary precipitate A is also known as ‘star shaped precipitate’. This forms during the solidification before eutectic reaction begins. It consists mainly of Al and Zn while the grey precipitate consists of Zinc mainly. The continuous matrix C which consists mainly of eutectic mixture of Sn and constitutes maximum of the volume fraction. The phase A accounting for the least volume percentage has a phase transition temperature higher than eutectic temperature in view of its high Al and Zn contents in comparing to that of the eutectic phase.

4.2.5 50Sn-43Zn-7Al (air cooled) solder alloy (sample 5)

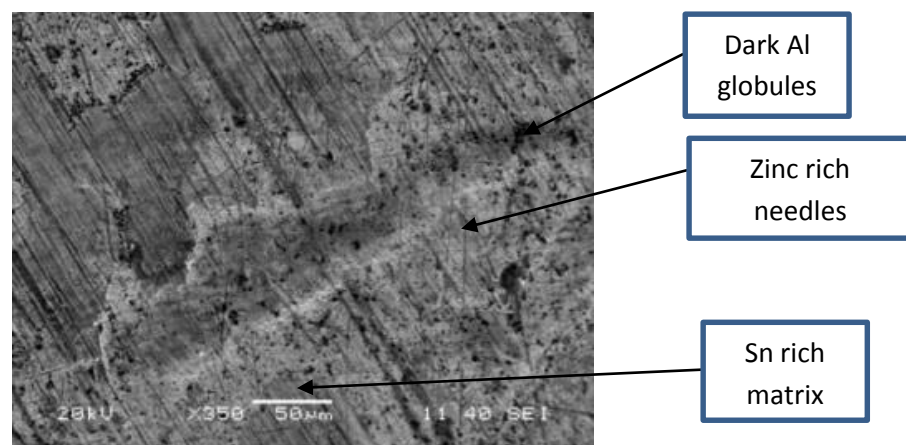


Figure 23-50Sn-43Zn-7Al (air cooled) solder alloy at low magnification

It is known that the solubility of Al in Sn is negligible and the solubility of Sn in Al is 0.025 at% at 300 °C. Here 7 at. % Al has been added but the at. % of Al in the matrix is only 1.62 %. This suggests that the excess Al segregates and precipitates in the Sn rich matrix and dark coloured spots. From this figure it is evident that there is decrease in the grain size and the increase in size and number of dark spots present which is because of the higher rate of cooling than in furnace cooled sample. Because of the higher rate of cooling than furnace cooling, the time for diffusion decreases and thus instead of forming platelets, elements segregates as a globules.

4.2.6 10Sn-80Zn-10Al (furnace cooled) solder alloy (sample 6)

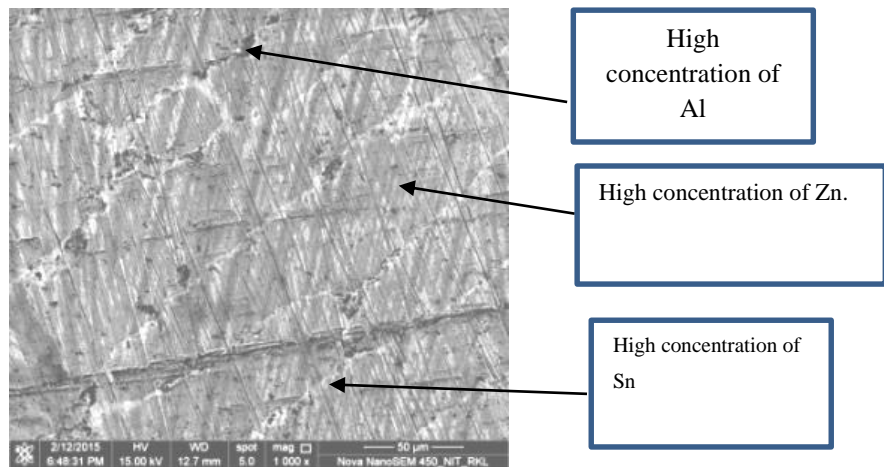


Figure 24-10Sn-80Zn-10Al (furnace cooled) solder alloy

In this figure we can clearly see grains and grain boundary. Since the sample is highly zinc rich we can clearly see that as the Grey matrix which is the Zn rich region. The white grain boundary region is highly sn rich. And the dark globules are Al rich. Since grain boundaries are the most active site in a specimen so Sn and Al segregation takes place at the grain boundary.

The three phases present here are as follows:-

- a. Small Black phase (A) – Small globules containing high concentration of Al + Zn along with oxygen.
- b. Grey phase (B) – Needle-like grey-coloured Zn-rich phase.
- c. White phase (C) –The white-coloured matrix also known as the β -Sn contains almost 100 % Sn with negligible amounts of Al and Zn.

4.2.7 10Sn-80Zn-10Al (air cooled) solder alloy (sample 7)

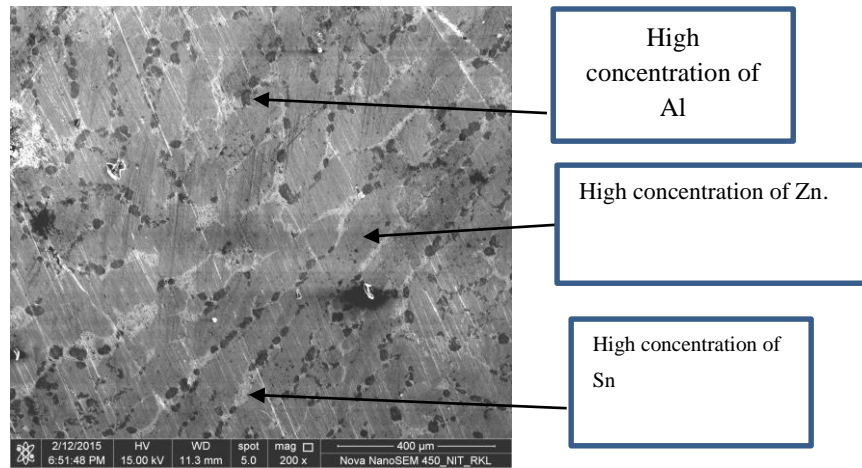


Figure 25-10Sn-80Zn-10Al (furnace cooled) solder alloy

In the air-cooled solder sample, the grains are much finer. We can also see the increase in the presence of the dark-coloured phase which is rich in aluminium. This is because of the higher rate of cooling which does not give time for diffusion of particles, and therefore, they precipitate quite quickly.

4.3 EDX Analysis

4.3.1 Sn- Zn Eutectic Alloy (sample 1)

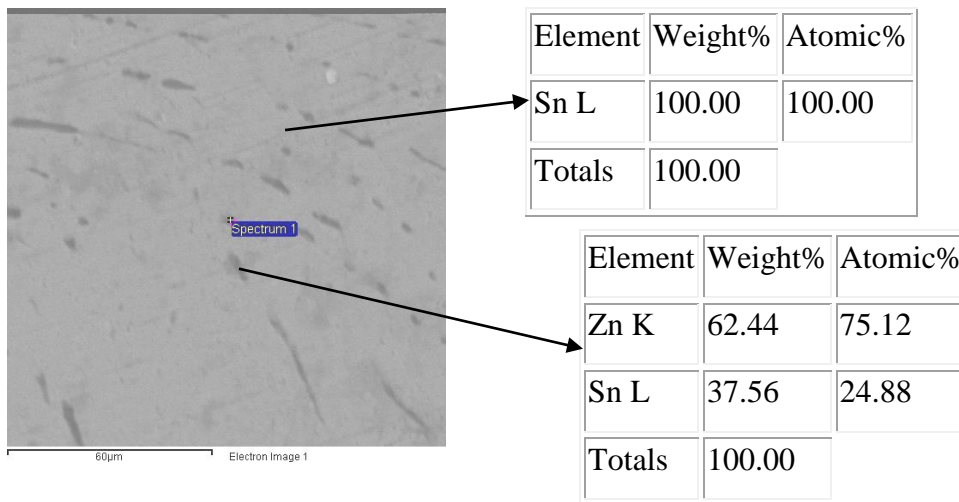


Figure 26- EDX analysis for Sn- Zn Eutectic Alloy

The EDX result of the Sn-Zn eutectic alloy indicates a typical lamella eutectic microstructure with homogeneous distribution of Zn rich platelets on Sn matrix.

4.3.2 82Sn-15Zn-3Al (Air cooled) solder alloy

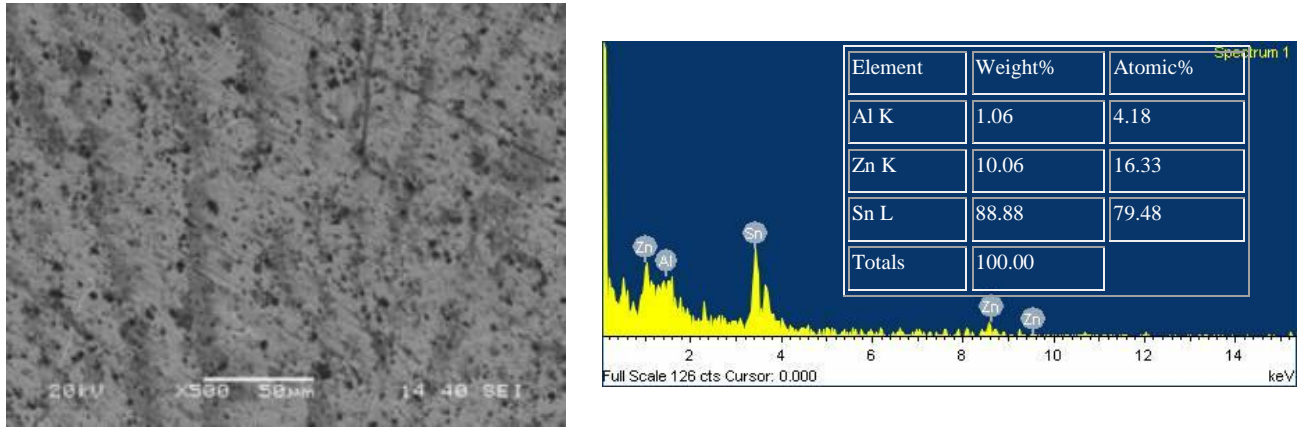


Figure 27-EDX analysis for 82Sn-15Zn-3Al (Air cooled) solder alloy

The EDX analysis suggests that the initial composition of 3Al-15Zn-82Sn has been maintained in the solder alloy. The air cooled microstructure shows a microstructure having more dense dark-coloured regions. The addition of low atomic % of Al (3 at. % Al) doesn't affect the microstructure of the alloy, and the resulting microstructure is highly similar to the microstructure of the Sn-14.9 at. % Zn (8.8wt. % Zn) eutectic alloy; the only difference is that it adds micro-inhomogeneity to the microstructure.

4.3.3 50Sn-43Zn-7Al (furnace cooled) solder alloy

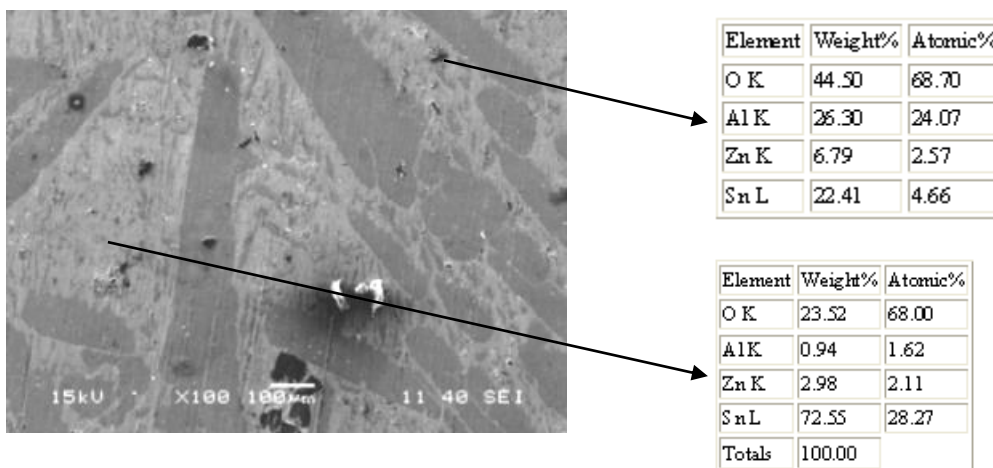


Figure 28-EDX analysis for 50Sn-43Zn-7Al (furnace cooled) solder alloy

It is evident from the EDX analysis of the various regions of the microstructure that the dark spots are Al-rich, the white regions containing the dark spots are Sn-rich, and the plane regions devoid of any dark spots are Zn rich. Al-Sn is a simple eutectic system with limited solid solubility in the two-terminal solid solutions (fcc (Al) and tetragonal (β Sn)). From the phase diagram of Al-Sn system, it is clear that Sn is negligibly soluble in Al. Sn has been observed to have a solubility of less than 0.01 wt.% in the Al at the melting point of approximately 231.2°C. Also, it is known that the solubility of Sn is approximately about 0.1% at a temperature of 600°C and above (Polmear, 1995). This is the reason that we see globules of dark-coloured Al in the Zn-rich region. They appear as small black dots in the Zn-rich regions.

4.3.4 10Sn-80Zn-10Al (furnace cooled) solder alloy

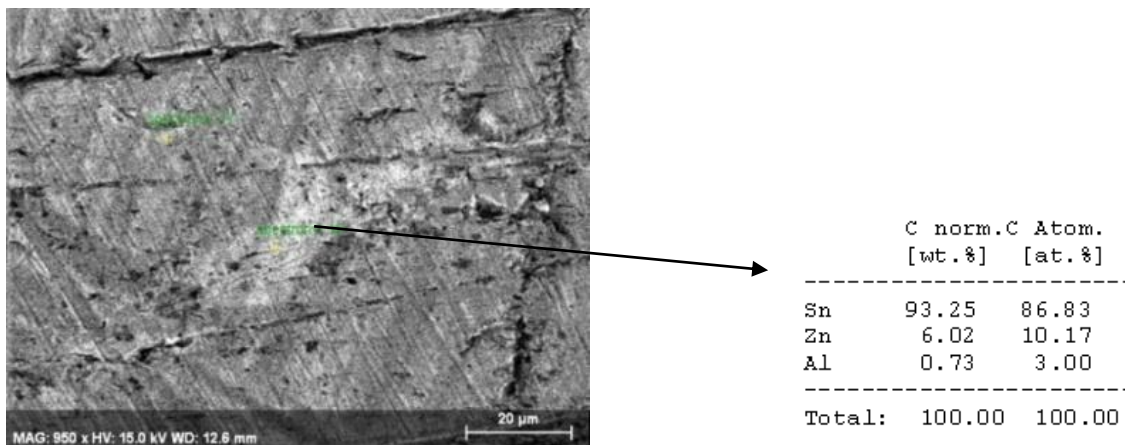


Figure 29-EDX analysis for 10Sn-80Zn-10Al (furnace cooled) solder alloy

4.3.5 10Sn-80Zn-10Al (air cooled) solder alloy

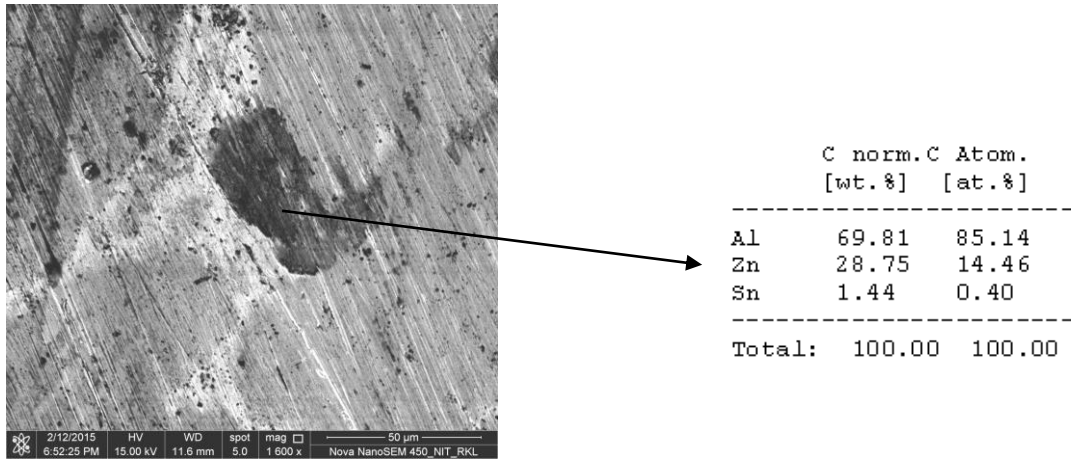


Figure 30-EDX analysis for 10Sn-80Zn-10Al (air cooled) solder alloy

The white regions in the microstructure are the Sn-rich regions with nearly-eutectic composition, whereas the dark black region is the Al-rich region which segregates in the form of small globules.

4.4 Thermal Analysis using DSC

4.4.1 Sn- Zn Eutectic Alloy (sample 1)

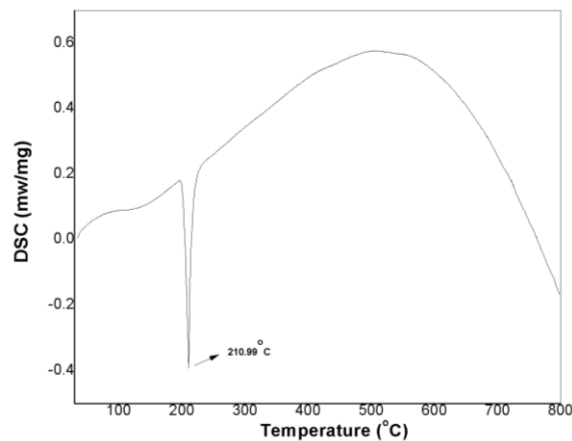


Figure 31-Thermal analysis by DSC for Sn- Zn Eutectic Alloy

The above DSC plot shows a sharp endothermic peak at around 211°C, which corresponds to the melting point of the eutectic solder alloy. Since the peak is very sharp so we can say that melting

takes place within a very small range, as it should be the case for an eutectic sample. The higher temperature might be due to the presence of inhomogeneities in the sample.

4.4.2 82Sn-15Zn-3Al (furnace cooled) solder alloy (sample 2)

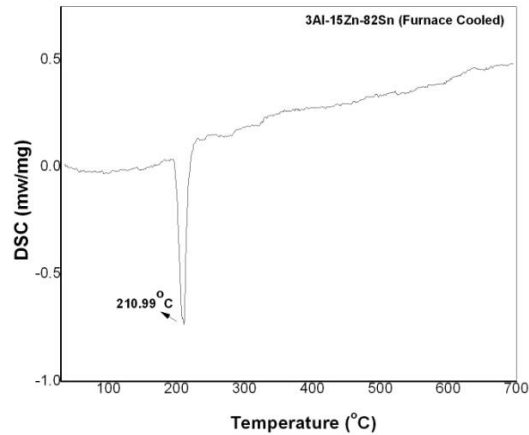


Figure 32- Thermal analysis by DSC for 82Sn-15Zn-3Al (furnace cooled) solder alloy

The DSC analysis in the above figure shows that the melting point of the furnace cooled 3Al-15Zn-82Sn alloy is 210.99°C. The melting point of this alloy is slightly higher than the melting point of the eutectic Sn-Zn composition (198°C). This might be possibly due to the small amount of Al that is added to the eutectic composition, or due to the presence of other impurities in the alloy.

4.4.3 82Sn-15Zn-3Al (Air cooled) solder alloy (sample 3)

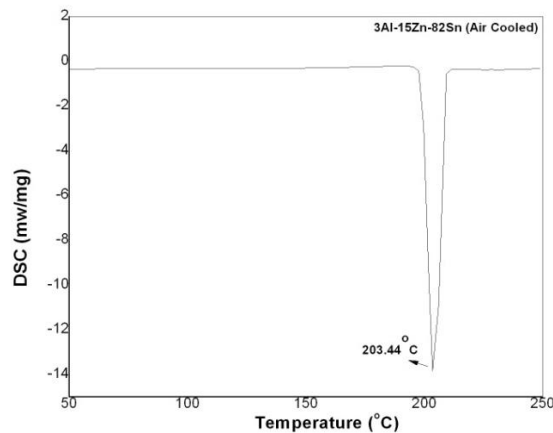


Figure 33- Thermal analysis by DSC for 82Sn-15Zn-3Al (furnace cooled) solder alloy

The melting point of the air cooled 3Al-15Zn-82Sn alloy is 203.44°C. The melting point of the air cooled alloy having the same composition is slightly lower than that of the furnace-cooled sample. The furnace cooled alloy having finer grain size has lower melting point due to higher surface area per unit volume.

4.4.4 50Sn-43Zn-7Al (furnace cooled) solder alloy (sample 4)

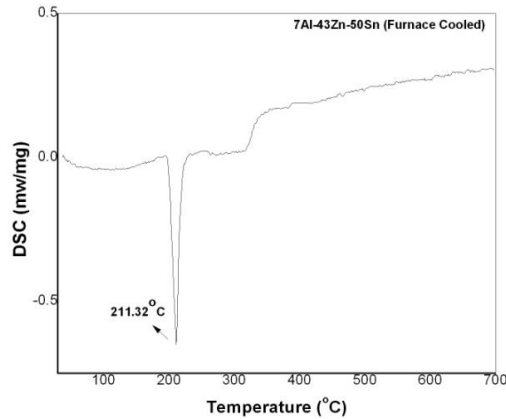


Figure 34- Thermal analysis by DSC for 50Sn-43Zn-7Al (furnace cooled) solder alloy

The melting point of this alloy is 211.32°C. This is higher than the melting point of sample-2, which may be due to the higher Al content, which results in the formation of a large number of globules, and thus the melting point increases slightly.

4.4.5 50Sn-43Zn-7Al (air cooled) solder alloy (sample 5)

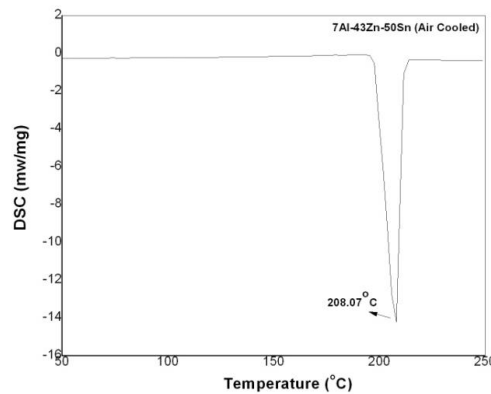


Figure 35- Thermal analysis by DSC for 50Sn-43Zn-7Al (air cooled) solder alloy

The melting point of the air cooled 50Sn-43Zn-7Al alloy is 208.07°C. The melting point of the air cooled alloy having the same composition is slightly lower than that of the furnace cooled sample. The furnace-cooled alloy having finer grain size has lower melting point due to the higher surface area per unit volume as is observed in sample-3.

4.4.6 10Sn-80Zn-10Al (furnace cooled) solder alloy (sample 6)

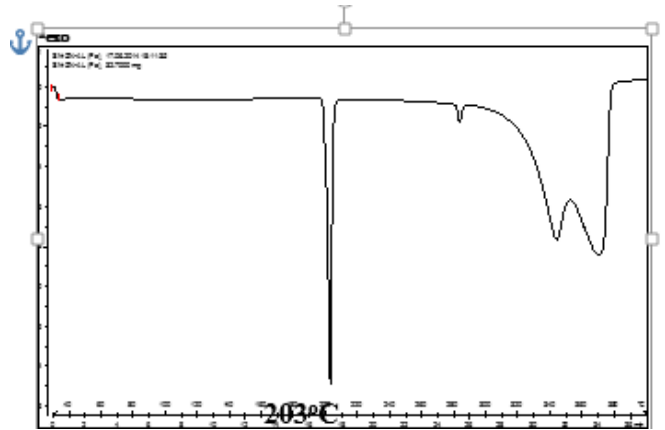


Figure 36- Thermal analysis by DSC for 10Sn-80Zn-10Al (furnace cooled) solder alloy

The initial endothermic peak may be due to melting of eutectic alloy at some region in the sample. The other endothermic peaks are possible due to the melting of Zn and Sn which did not go into solid solution. It should be noted that this is the composition which is farthest from the eutectic composition. The Al-Zn phase diagram shows a eutectoid reaction at around 277°C. The small endothermic peak at around 281°C in the DSC plots is possibly due to the eutectoid reaction. The Al-Zn eutectic temperature is 381°C. So the endothermic peak at around 370°C is possibly due to the melting of the Al-Zn eutectic composition. The composition of 10Al / 80 Zn / 10Sn is very close to the Al-88.7 atomic % Zn eutectic composition. So there is possibility of formation of the eutectic Al-Zn alloy. This is also evident from the SEM and EDX analysis.

4.4.7 10Sn-80Zn-10Al (air cooled) solder alloy (sample 7)

The air cooled sample shows deeper endothermic peaks compare to the furnace cooled as in the case of furnace cooled alloy there is more diffusion taking place resulting more eutectic phase and leaving behind a lesser amount of pure elements in the solder alloy.

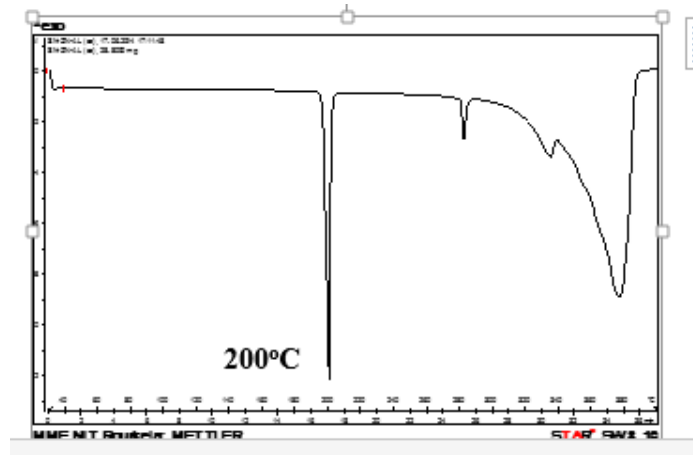


Figure 37- Thermal analysis by DSC for 10Sn-80Zn-10Al (air cooled) solder alloy

As we go away from the eutectic composition of Sn-8.8wt. % Zn or 14.9 at. % Zn we do not get a single melting point of the alloy as seen in the case of 10Al / 80Zn / 10Sn [wt.%]. This is also evident from the DSC plot of 7Al/43Zn/50Sn sample where a small endothermic peak at around 300-400°C is seen after the melting of the eutectic composition at 211.32°C.

4.4.8 Comparison of melting points of different solder alloy compositions

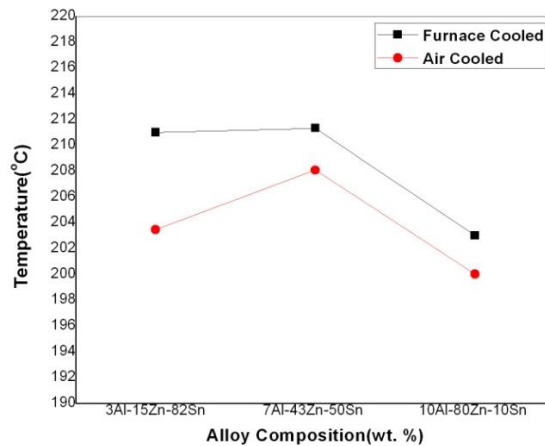


Figure 38-Variation of melting points with different compositions and cooling conditions

When we move from 3 Al to 7 Al, there is not much appreciable increase in the melting point (the increase is due to the higher Al content, which has a higher melting point). On the other hand, when we move from 7 Al to 10 Al, we observe a steep fall in the melting temperatures. This may be because of the following reasons:-

1. There may be formation of other compounds (possibly eutectic) with Al; these might have a lower melting point.
2. The matrix in this case is Zn rich, as compared to the previous cases.
3. As in the case of this solder alloy, we have moved farther away from the eutectic composition, so there may be interactions between inhomogeneities and constituent elements.

4.5 Oxidation Analysis using TGA

4.5.1 Sn- Zn Eutectic Alloy (sample 1)

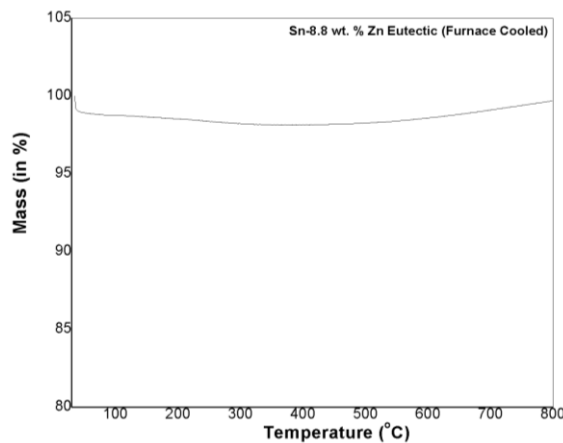


Figure 39-TGA of Sn- Zn Eutectic Alloy

The overall mass increase in eutectic sample is around 1%. This is due to the fact that with an increase in temperature (in atmospheric conditions), the sample gets oxidised, and thus the weight of the specimen will increase.

4.5.2 82Sn-15Zn-3Al (furnace cooled) solder alloy (sample 2)

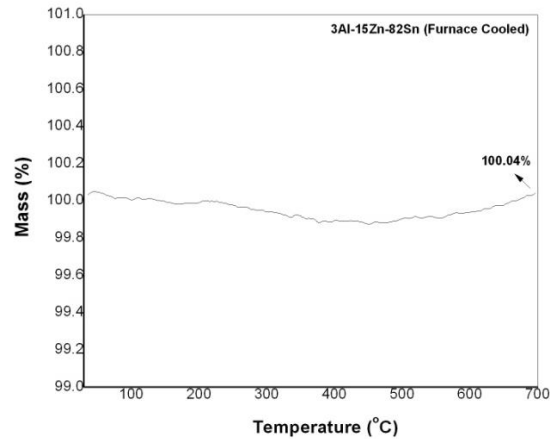


Figure 40-TGA of 82Sn-15Zn-3Al (furnace cooled) solder alloy

There is a very slight increase in the weight, which may be due to the oxidation of Al. As Aluminium is very prone to oxidation, thus it readily forms an Al_2O_3 oxide layer, and therefore the increase in mass is observed.

4.5.3 82Sn-15Zn-3Al (Air cooled) solder alloy (sample 3)

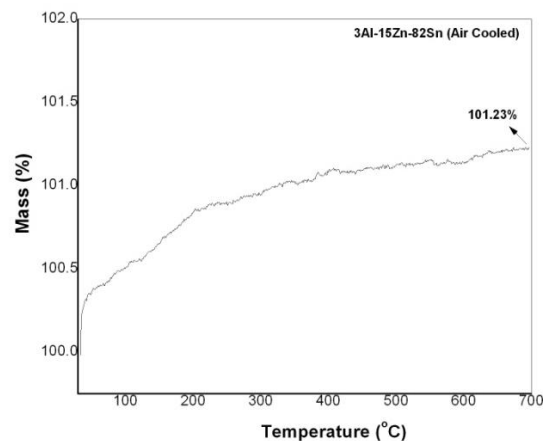


Figure 41-TGA of 82Sn-15Zn-3Al (Air cooled) solder alloy

As is evident from the curve, the mass increase in air-cooled sample is much more than the mass increase in the furnace-cooled sample, which may be due to the fine grain structure leading to increase in surface area, and as a result, higher oxidation.

4.5.4 50Sn-43Zn-7Al (furnace cooled) solder alloy (sample 4)

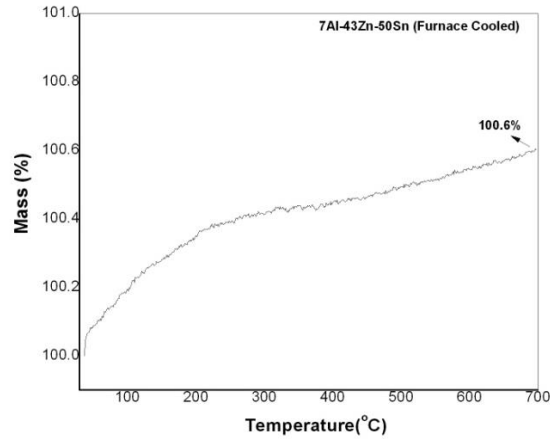


Figure 42-TGA of 50Sn-43Zn-7Al (furnace cooled) solder alloy

The increase in mass is about 0.6%, which is higher than the increase in mass in the furnace-cooled 3 Al sample. This may be because of the presence of higher Al content which leads to the increase in oxidation of Aluminium owing to its higher affinity towards oxygen as compared to Zn and Sn.

4.5.5 50Sn-43Zn-7Al (air-cooled) solder alloy (sample 5)

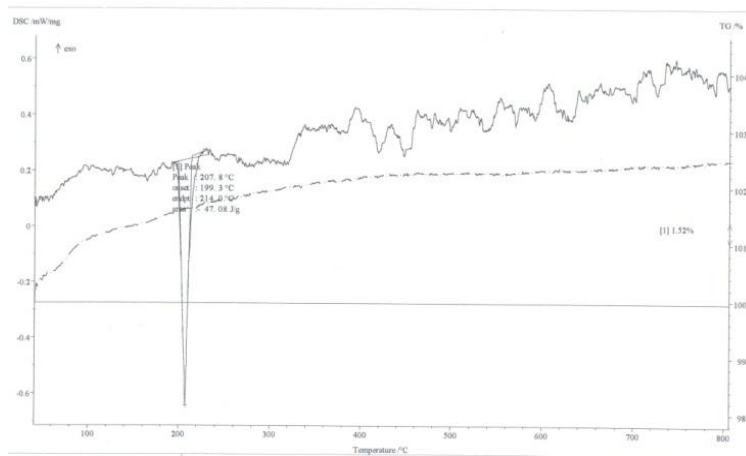


Figure 43-TGA of 50Sn-43Zn-7Al (air-cooled) solder alloy

The mass increase in this sample is about 2.5% which is much high than both the 7Al (furnace cooled) and the 3Al (air cooled) samples. This may be because of the higher surface area in air-cooled sample in comparison to the furnace-cooled sample, and also because of the high Aluminium content.

4.5.6 10Sn-80Zn-10Al (furnace cooled) solder alloy (sample 6)

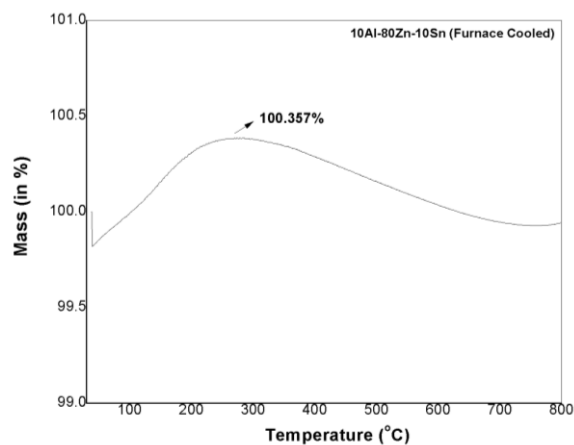


Figure 44-TGA of 10Sn-80Zn-10Al (furnace cooled) solder alloy

The trend of increase in mass with an increase in the Al content is not followed in this sample. This may be due to the formation of an oxide layer of Al which completely covers the sample and does not let any other element (Sn & Zn) to get oxidised. So the mass increase is only due to the formation of Aluminium Oxide film, which might not have been the case when Aluminium content was less than 10%. Since in these samples the Al content may not be high enough to form an oxide film which covers the sample completely, thus there might have been oxidation of Sn & Zn which led to higher mass increase.

4.5.7 10Sn-80Zn-10Al (air cooled) solder alloy (sample 7)

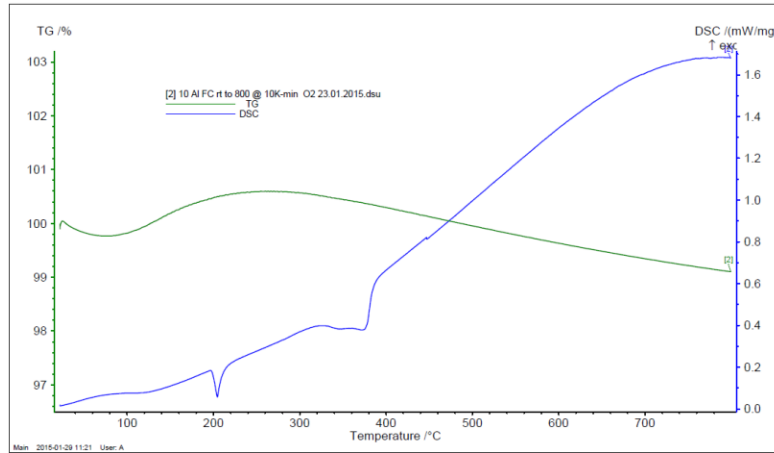


Figure 45-TGA of 10Sn-80Zn-10Al (air cooled) solder alloy

The initial decrease in the air-cooled sample may be due to the absorbed water in the sample. Thereafter the rise in the TGA curve is due to the oxidation of the solder alloy. Here also, the mass increase is higher than the furnace-cooled sample with the same composition because of higher available surface area.

To summarise, initially, there is sharp increase in weight, as indicated by the initial steep slope in the TGA curve. This may be due to the fast formation of Aluminium oxide. On progressive increase in Al content, there is the formation of an Al_2O_3 film. The formation of the film is complete by $\sim 220^\circ\text{C}$, beyond which the rate of formation of Al_2O_3 reduces as indicated by the decrease in the slope of the TGA curve. Beyond this temperature, the rise in mass is very slow and negligible. This slope is not visible in the TGA of the Sn-Zn eutectic sample. Therefore, addition of Al can prevent the oxidation of the Sn-Zn solder alloy by forming an Al_2O_3 layer.

4.6 Wettability of the Solder on the Cu Substrate

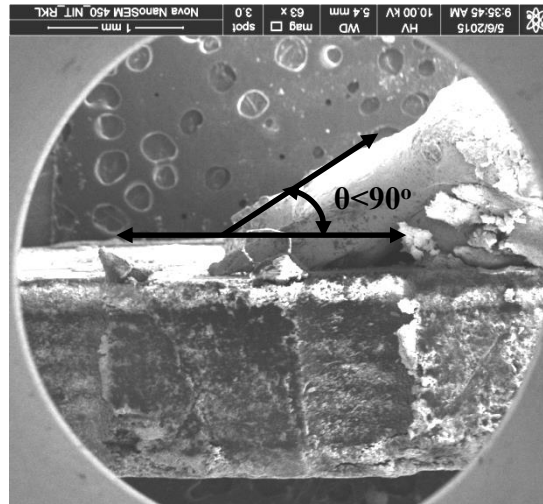


Figure 46- SEM Image showing contact angle of Sn-Zn Eutectic Solder alloy.

Wettability of a sample is measured by the contact angle which the solder alloy makes with the Cu substrate. Higher the contact angle, lesser will be its wettability.

The Sn-Zn eutectic sample has the lowest wettability with the highest contact angle and with increase in Al content the contact angle decreases, thereby resulting in an increase in the wettability.

As Zinc absorbs oxygen on the surface and forms a porous ZnO layer. This oxide layer thickness increases as the oxidation continues. So, the wetting power of the solder decreases significantly. However, when Aluminum atoms are added in place of the Zinc, the Aluminum atoms come in contact with the air, and the formation of a dense Al_2O_3 layer takes place preferentially. It is known that Aluminum atoms are prone to release electrons partially due to their chemical properties and react with oxygen molecules. The segregation of Al atoms in the solder prevents the reaction of Zn with oxygen. Electron releasing Al atoms are constantly provided to the metal surface. However, adding very high Al wt. % to the Sn-Zn solder alloy could make the solder brittle and reduce its wettability on the Cu substrate. This might be due to the formation of an Al_2O_3 layer, and the agglomeration of Al powders on the alloy surface. Therefore, adding up to 7 atomic wt. % of Al could give the desired oxidation resistance to the solder alloy without harming its wettability.

CHAPTER-5

CONCLUSIONS

To summarize,

1. All the samples were successfully developed, and tested to determine their characteristics and properties.
2. In the 3 Al-15 Zn-82 Sn alloy, we observe a Sn-rich matrix, on which needle-like Zn-rich phase is seen. There is some segregation of Al, which we can observe as black dots. In the 7Al-43 Zn-50 Sn solder alloy, we observe the following three phases:
 - a. Small Black phase (A) – Small globules containing high concentration of Al + Zn along with oxygen.
 - b. Grey phase (B) – Needle-like grey-coloured Zn-rich phase.
 - c. White phase (C) –The white-coloured matrix also known as the β -Sn contains almost 100 % Sn with negligible amounts of Al and Zn.
 - d. We observe similar phases in 10Al- 80 Zn-10 Sn solder alloy too, but in 10Al- 80 Zn-10 Sn solder alloy, the Zn-rich grey phase acts as the matrix. The white-coloured Sn-rich phase is present in the grain boundaries. Dark-coloured Al-rich globules could also be seen in the microstructure of the solder alloy.
3. The EDX analysis suggests that the initial composition of 3Al-15Zn-82Sn has been maintained in the solder alloy. The air cooled microstructure shows a microstructure having denser needle-like grey-coloured phases. For the 7Al-43Zn-50Sn alloy, it is evident from the EDX analysis of the various regions of the microstructure that the dark spots are Al-rich, and the white region is the Sn-rich matrix. The matrix is almost 100 % Sn. The grey-coloured needle like phases are Zn rich (6.79 wt. % Zn and 22.41wt.% Sn) . For the 10 Al-80 Zn-10 Sn solder alloy, the white regions in the microstructure are the Sn-rich regions. The white coloured Sn-rich phase could be seen in the grain boundaries. The dark coloured Zn rich phase is the matrix in the case of 10 Al- 80 Zn-10 Sn solder alloy.
4. As the concentration of Al rises from 3 to 7 at. %, there is not much appreciable increase in the melting point of the alloy. The slight increase in melting point of the solder alloy is due to the higher Al content which has a higher melting point (660 °C). On the other hand, when the Al concentration is raised from 7 to 10 at. % Al, we observe a steep fall in the melting temperatures. This may be because of the following reasons:
 - a. As the Al concentration is higher there may be formation of other phases (possibly eutectic) with Al. These phases might have a lower melting point.

- b. The matrix in this case is Zn rich, as compared to the previous cases.
 - c. As in the case of this solder alloy, we have moved farther away from the eutectic composition, so there may be interactions between inhomogeneities and constituent elements.
5. The TGA analysis of most of the solder alloys show that initially, there is sharp increase in mass. This is indicated by the initial steep slope in the TGA curve. This may be due to the fast formation of aluminium oxide. On progressive increase in Al content, there is the formation of an Al₂O₃ film. The formation of the film is complete by ~220°C, beyond which the rate of formation of Al₂O₃ reduces as indicated by the decrease in the slope of the TGA curve. Beyond this temperature, the rise in mass is very slow and negligible. This slope is not visible in the TGA of the Sn-Zn eutectic sample. Therefore, addition of Al could prevent the oxidation of the Sn-Zn solder alloy by forming an Al₂O₃ layer.

Thus, we conclude

- **Thermo Gravimetric analysis (TGA)**-Formation of Al₂O₃,and its effect:
 - Increasing corrosion resistance
- **Melting point**
 - When at. % for Al increases from 3 to 7, there is slight increase in the melting point, but it falls as at. % increases to 10
 - Melting point for air-cooled samples is lesser than that for furnace-cooled samples
- **Wettability**
 - Increases with increasing Al content, but for 10 Al (at. %), due to high powder segregation and thick Al₂O₃ layer, the solder alloy becomes brittle
- *Taking the afore-mentioned factors into consideration , we conclude that the solder alloy containing 7 Al (at. %) is the most suitable sample for use in soldering purposes.*

REFERENCES

1. S. Vaynman, G. Ghosh and M. E. Fine, *Some Fundamental Issues in the Use of Zn-Containing Lead-Free Solders for Electronic Packaging*, *Materials Transactions, Special Issue on Lead-Free Soldering in Electronics, The Japan Institute of Metals*, Vol. 45, No. 3 (2004) pp. 630 to 636
2. R. C. Dorward, *The solubility of tin in aluminium*, *Metallurgical Transactions A*, 1976, 7A, 308-310
3. *Materials Transactions*, Vol. 51, No. 10 (2010) pp. 1747 to 1752
4. *Special Issue on Lead-Free and Advanced Interconnection Materials for Electronics*
5. *The Japan Institute of Metals Effect of Small Addition of Zinc on Creep Behavior of Tin* Naoyuki Hamada, Masakazu Hamada, Tokuteru Uesugi, Yorinobu Takigawa² and Kenji Higashi
6. *The Al-Sn(Aluminium-Tin)System*, A.J.McAlister and D.J.Kahan, *National Bureau of Standards, Bulletin of Alloy Phase Diagrams* Vol. 4 (4) 1983. Page 410.
7. M. Hansen, *Constitution of Binary Alloys*, second ed., McGraw-Hill Book Co., New York, 1958.
8. J.L. Murray, *Bull. Alloy Phase Diagrams* 4 (1983) 55–126.
9. K.L. Lin, L.H. Wen, T.P. Liu, *J. Electron. Mater.* 27 (1998) 97–105
10. *Development of Lead-free solders*, Masayuki Katajima and Tadaki Shono, *FUJITSU Sci. Tech.* (July 2005).
11. *Formation of intermetallic compounds at eutectic Sn–Zn–Al solder/Cu interface*, Shan Pu-Yu, Moo- Chin Wang, Min-Hsiung Hon, *Journal, Materials Research Society* (Vol. 16, Jan 2001).
12. *Study Of Zn – Sn – Al Alloys For High-Temperature Solders*, Prof.Ing. Jaromír Drápala, Aleš Kroupa, Ing. Bedřich Smetana, Ing. Rostislav Burkovič, Doc. Ing. Stanislav Lasek, Bc. Jan Musiola, *Hradec nad Moravicí* (21.05.2008).
13. *The Microstructures of the Sn-Zn-Al Solder Alloys*, KWANG-LUNG LIN, LI-HSIANG WEN, and TZY-PIN LIU, *Journal of Electronic Materials*, Vol 27.
14. *Study on melt properties, microstructure, tensile properties of low Ag content Sn–Ag–Zn Lead-free solders*, Tingbi Luo, Zhuo Chen, Anmin Hun, Ming Li, *Materials Science and Engineering A* 556 (2012) 885-890.

15. Resonant vibration behavior of Sn–Zn–Ag solder alloys, J.M. Song, T.S. Lui, G.F. Lan, L.H. Chen, *Journal of Alloys and Compounds* 379 (2004) 233–239.
16. Microstructures of eutectic Sn–Ag–Zn solder solidified with different cooling rates, C. Wei, Y.C. Liu, Y.J. Han, J.B. Wan, K. Yang, *Journal of Alloys and Compounds* 464 (2008) 301–305 (Sept. 2007)
17. Thermoelectric characteristics and tensile properties of Sn–9Zn–xAg lead-free solders, Fei-Yi Hung*, Chih-Jung Wang, Sung-Min Huang, Li-Hui Chen, Truan-Sheng Lui, *Journal of Alloys and Compounds* 420 (2006) 193–198 (December 2005).
18. Effects of small additions of Ag, Al, and Ga on the structure and properties of the Sn–9Zn eutectic alloy, Kang-I Chena, Shou-Chang Chenga, Sean Wu Kwang-Lung Lin, *Journal of Alloys and Compounds* 416 (2006) 98–105 (Sept. 2005).
19. The Microstructures of the Sn-Zn-Al Solder Alloys, KWANG-LUNG LIN, LI-HSIANG WEN, and TZY-PIN LIU, *Journal of Electronic Materials*, Volume 27, 1998.
20. A Thermodynamic Analysis Of The Al-Zn System and Phase Diagram Calculation, Shuang-Lin Chen And Y. A. Chang, *Calj'halj* Vol. 17, No. 2, Pp. 113-124, 1993.
21. Microstructure of Al-Zn and Zn-Al Alloys, Željko Skoko,^a Stanko Popović,^{a,**} and Goran Štefanić^b, *CROATICA CHEMICA ACTA* (Dec, 2008).
22. Soldering Properties of Sn-Zn-X Micro Solder Powders Fabricated by Melts Dispersion Technique, J. I. Youn, W. Ha, Y. J. Kim, "Soldering Properties of Sn-Zn-X Micro Solder Powders Fabricated by Melts Dispersion Technique", *Advanced Materials Research*, Vols 15-17, pp. 995-1000, Feb. 2006.
23. Mechanism of Interaction ($\leq 300^\circ\text{C}$) between Aluminum and Moist Sn and Its Alloys, CHEN Rong; ZHANG Qiyun (Department of Chemistry, Peking University, Beijing, 100871)